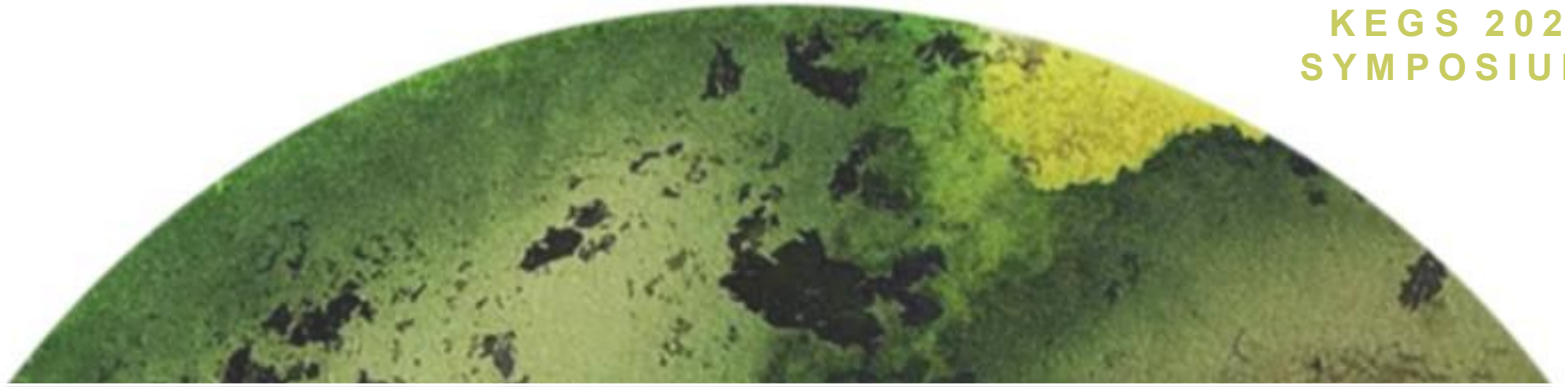

MAGNETOTELLURICS IN A CHALLENGING ENVIRONMENT

ALAN G. JONES*[1], JOEL JANSEN[2], RANDALL MACKIE[3], STEFANO GARANZINI[3], ERHAN ERDOGAN[4], YANN AVRAM[4], JAREN STRANDLIE[5]

1: MANOTICK GEOSOLUTIONS LTD., MANOTICK, ONTARIO, CANADA
2: LUNDIN MINING CORPORATION, VANCOUVER, BRITISH COLUMBIA, CANADA
3: VIRIDIEN, MILAN, ITALY
4: PHOENIX GEOPHYSICS, TORONTO, ONTARIO, CANADA
5: TALON NICKEL (USA) LLC, TAMARACK, MINNESOTA, USA

Eagle Mine MT Project – Overarching objective

Eagle Mine, located in Michigan's Upper Peninsula, is a small, high-grade underground nickel–copper mine and the only primary nickel producer in the USA

Overarching objective: Image possible deep basin and basement structures to the east of the existing mine with the objective of extending mine life by targeting deep basin-to-basement mineralization

Eagle Mine – Geology & Economics

The orebody is a magmatic Ni–Cu sulphide deposit associated with the ~1.1 Ga Mid-Continent Rift. Mining began in 2014, with projected production of ~440 Mlb Ni and ~429 Mlb Cu, plus minor Co, PGE, Ag, and Au, over a mine life currently expected to extend into the mid-2020s (Eagle Mine, 2026).

early cartoon

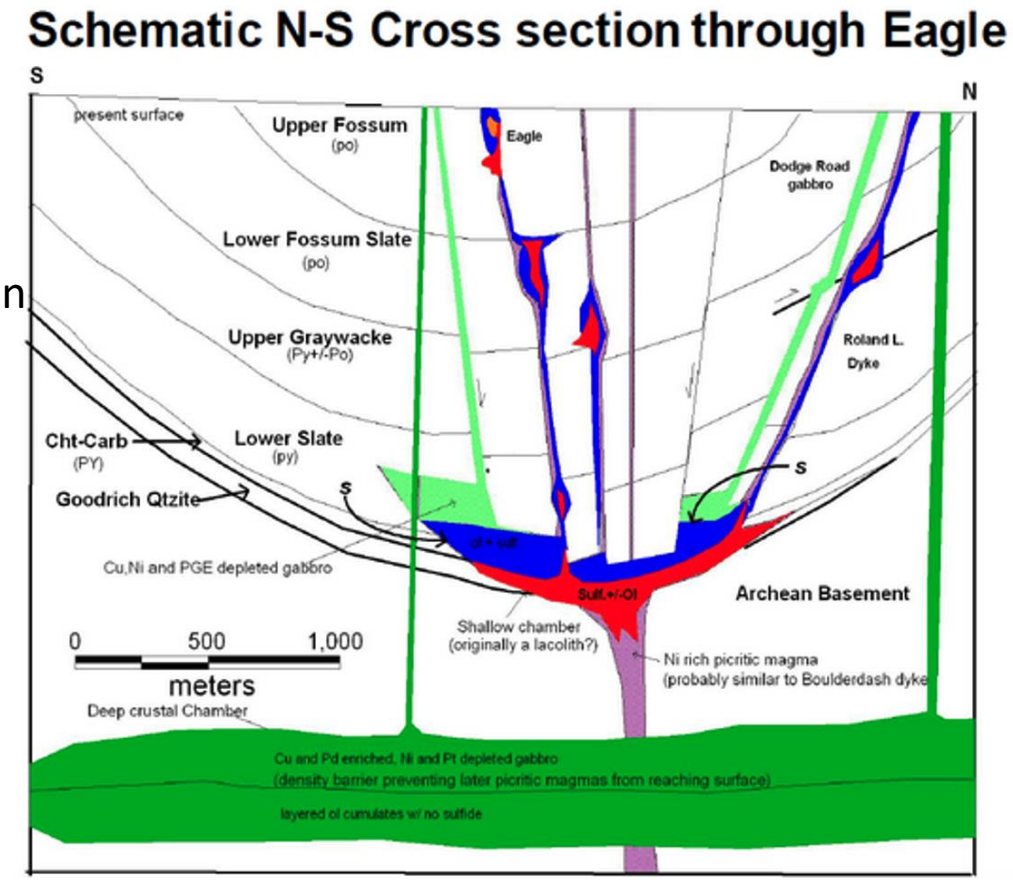

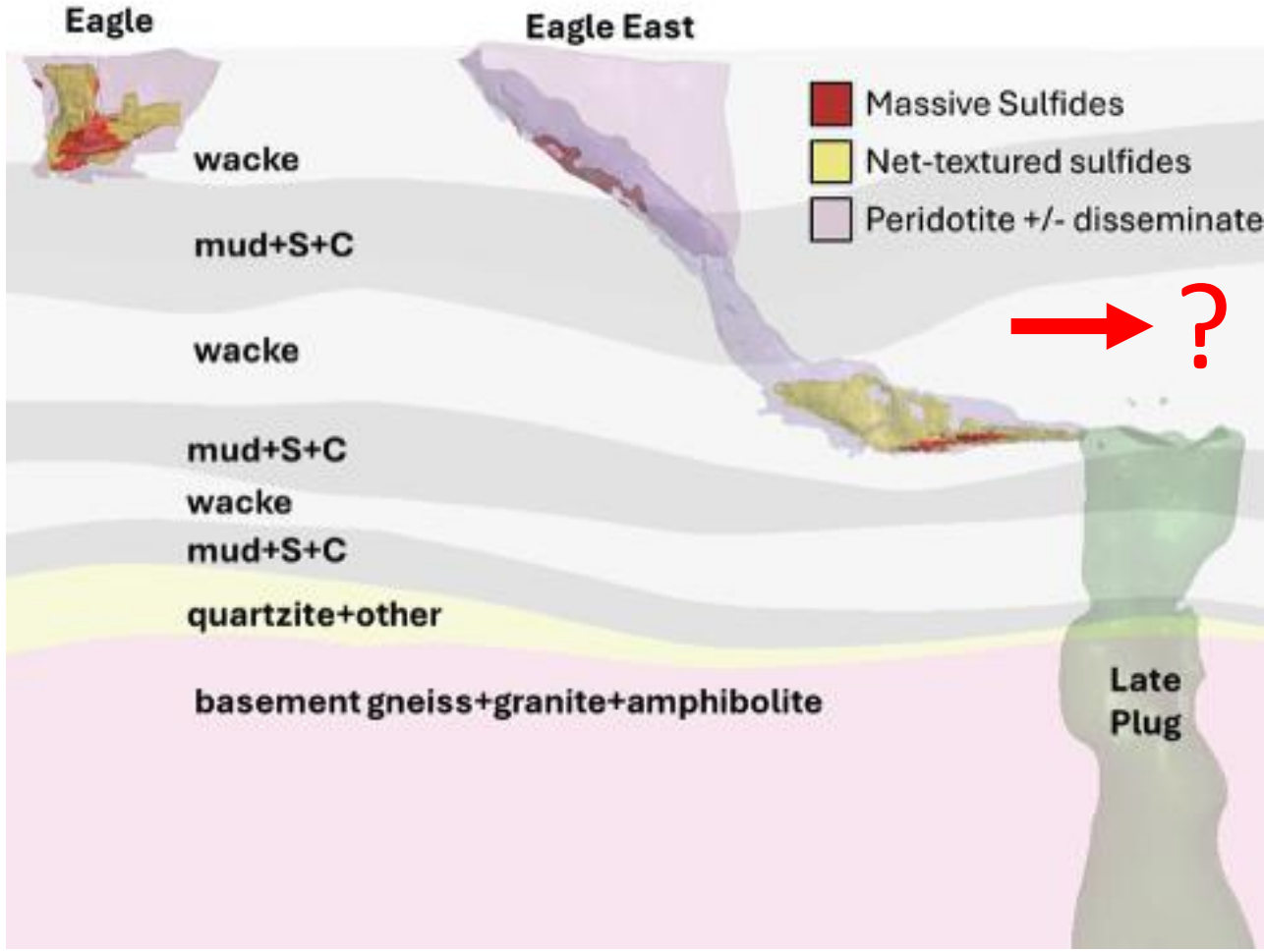

Eagle Mine MT Project Timeline

30/08/2022 – 01/10/2022 – Phase 0: Analysis and anisotropic 1-D inversions of 2007 Geosystem data

17/11/2022 – 26/04/2023 – Phase I: Acquisition, real-time assessment, survey re-design (06-27/11); Processing; Analysis of Phase I data; 3-D inversion of Phases 0+I data

26/04/2023 – 02/08/2023 – Phase II: Acquisition, real-time assessment, survey re-design; Processing; Analysis of Phase I data; 3-D inversion of Phases 0+I+II data

26/10/2023 – 14/02/2024 – Phase III: Acquisition, real-time assessment, survey re-design; Processing; Analysis of Phase I data; 3-D inversion of Phases 0+I+II+III data

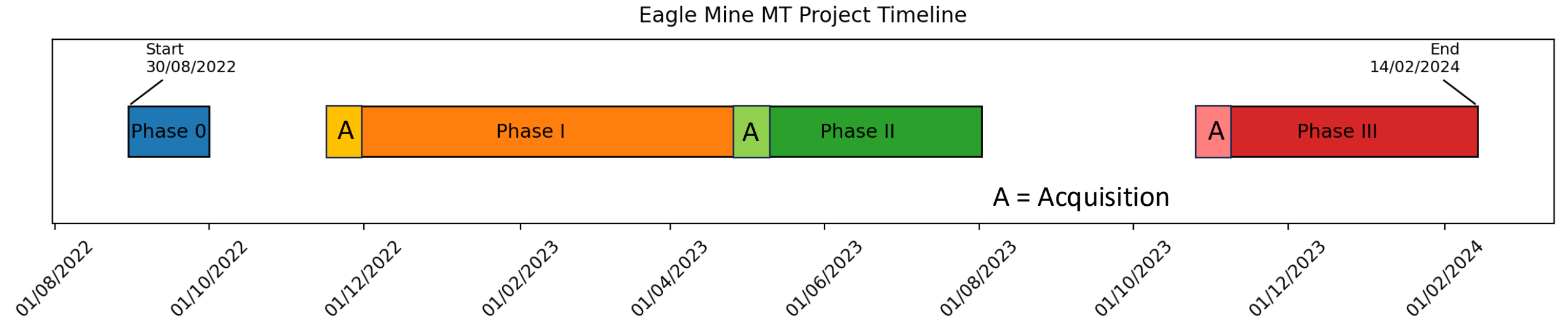

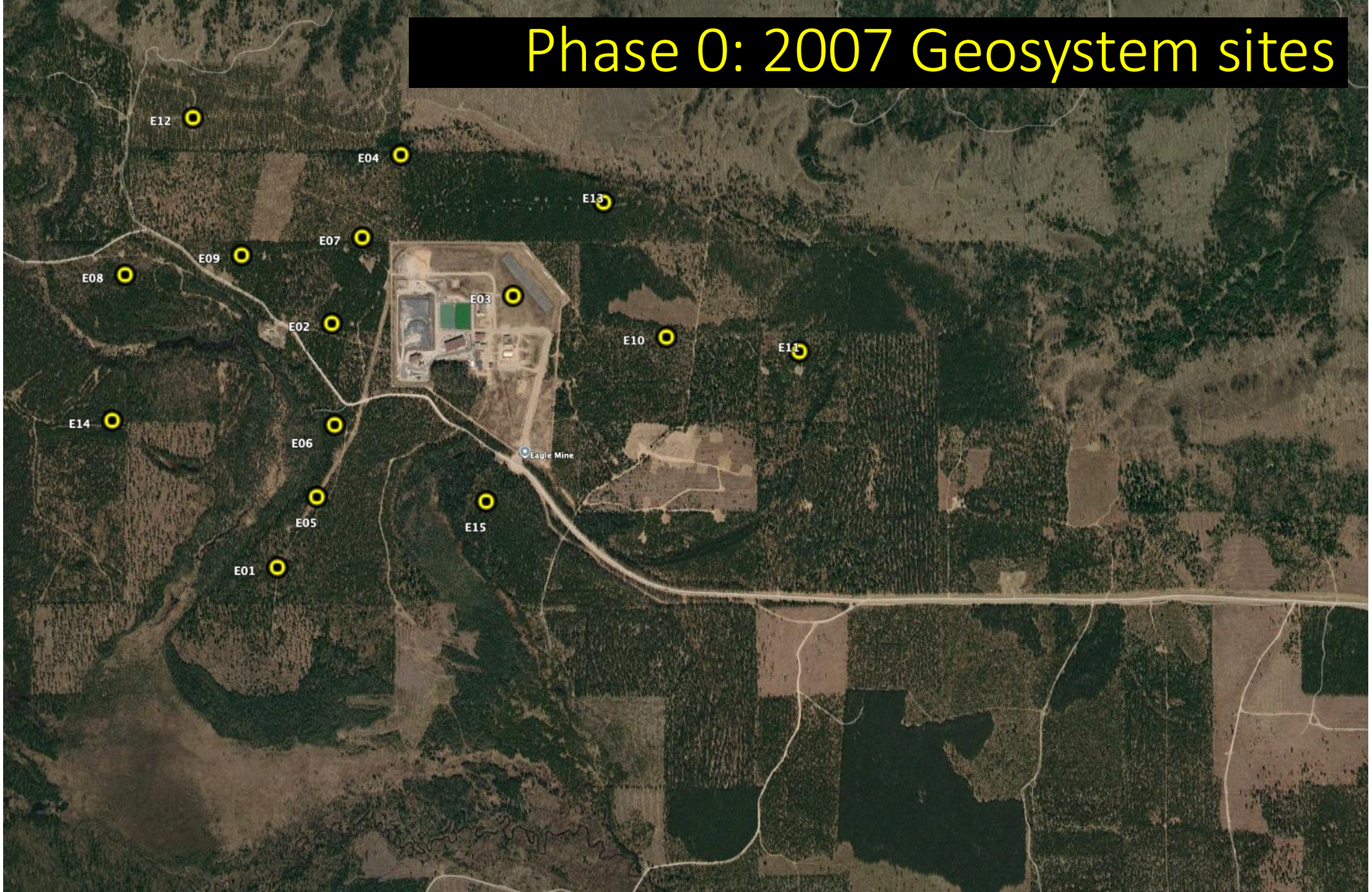
Phase 0: 2007 Geosystem sites
E12
E04
E13
E07
E09
E08
E03
E02
E10
E11
E14
E06
Eagle Mine
E05
E15
E01

Phase I: Phoenix Nov 2022 sites
Broad coverage of eastern ground

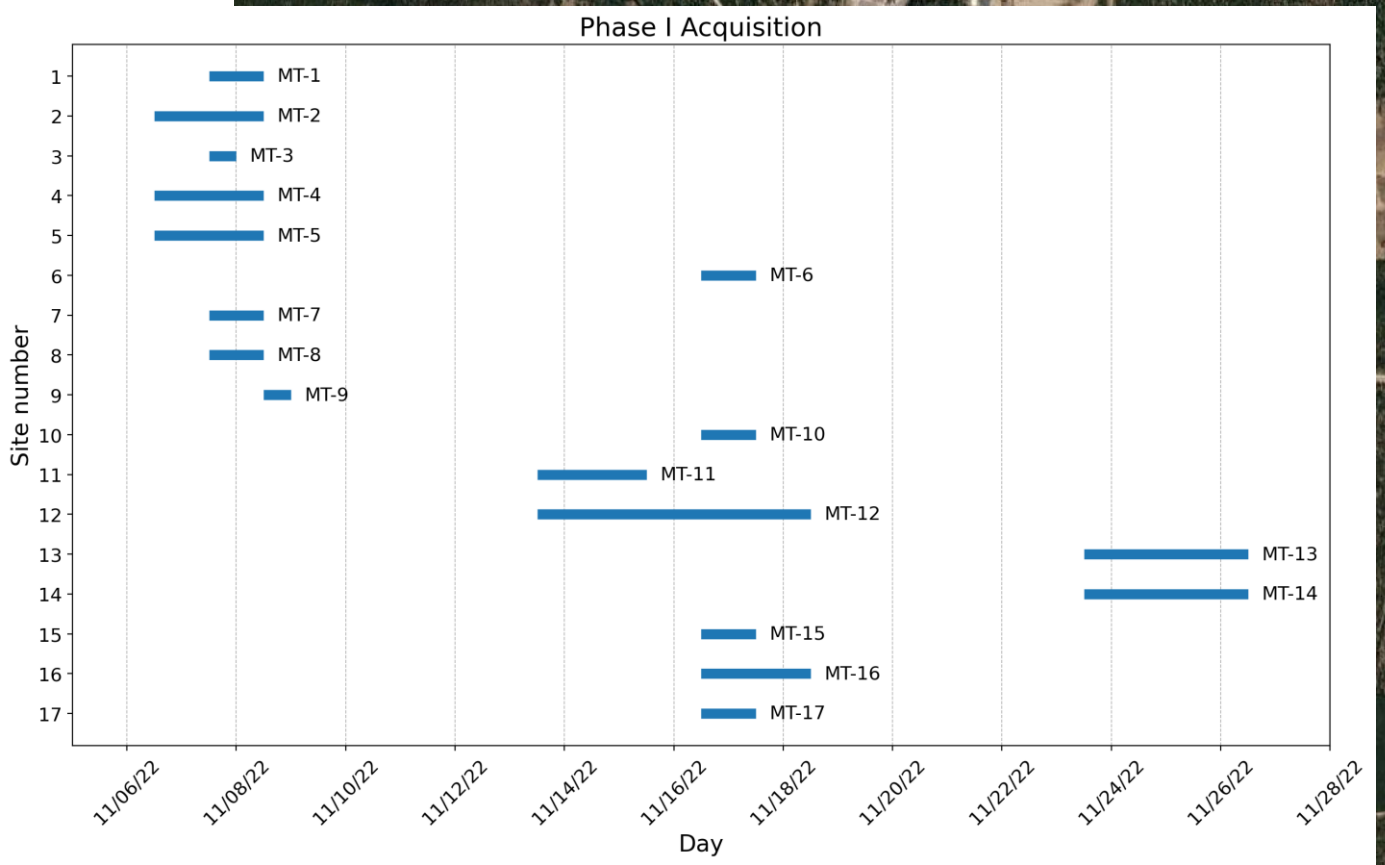

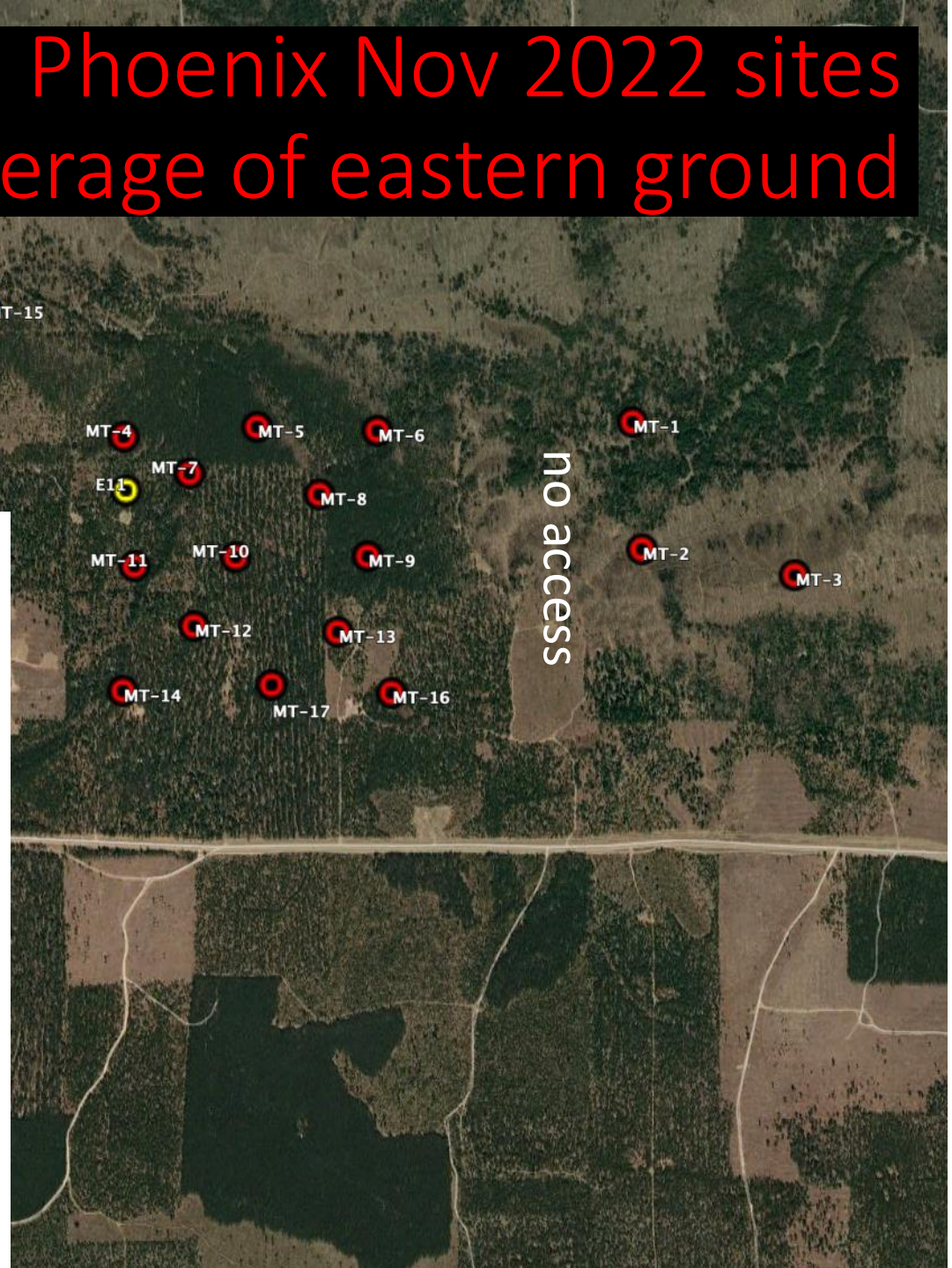

Phase II: Phoenix April 2023 sites
Higher density in centre

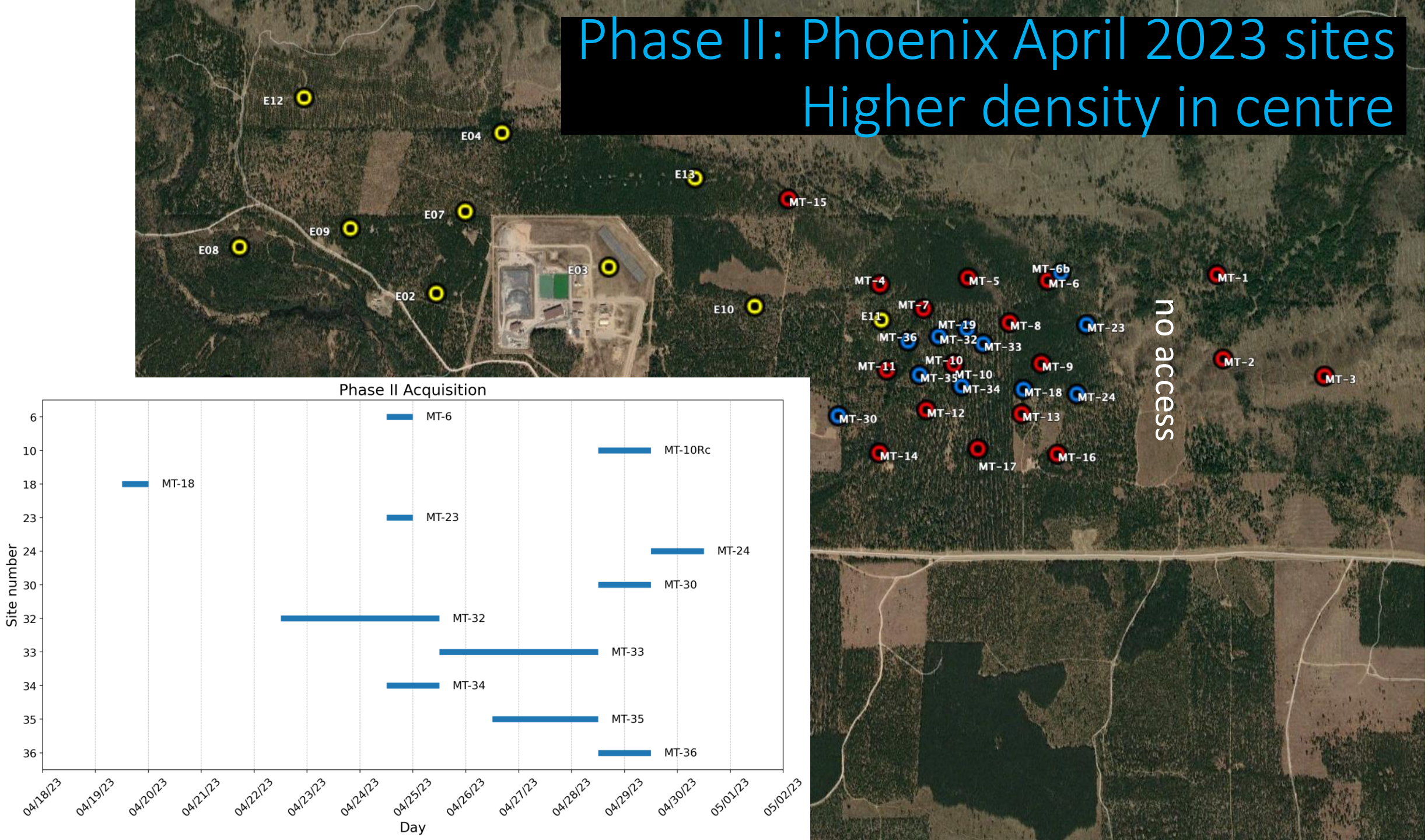

Phase III: Phoenix Oct/Nov 2023 sites
Investigate ground to the South

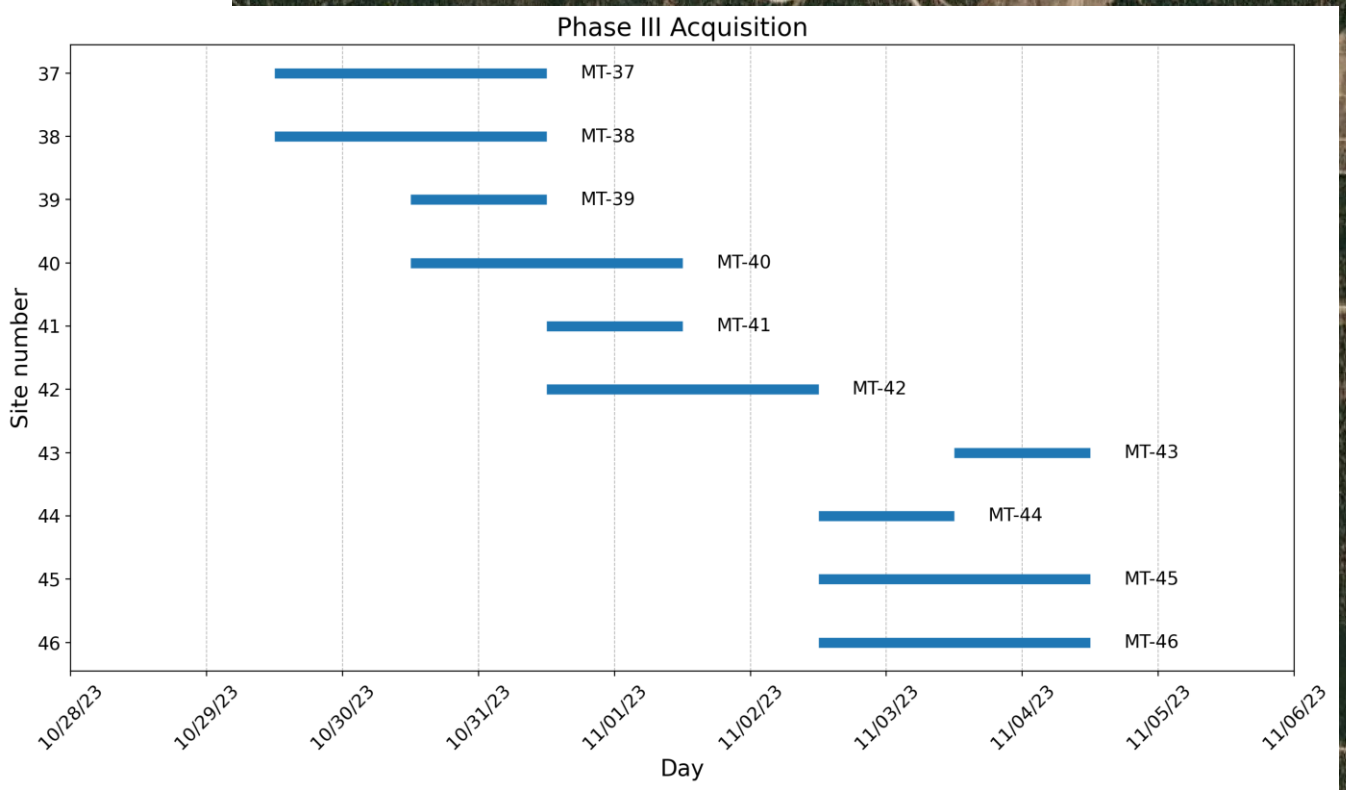

Acquisition - Equipment

Phoenix Geophysics acquisition using MTU-5C receivers, ultra-wideband MTC-150 coils, Pb-PbCl electrodes, 5 components at all sites

Phase I: standard electric field 5 electrode X-configuration, 100m dipoles

Phases II & III: enhanced electric field 17 electrode X-configuration, effectively “400m” dipoles, in response to 2022 low frequency response estimates

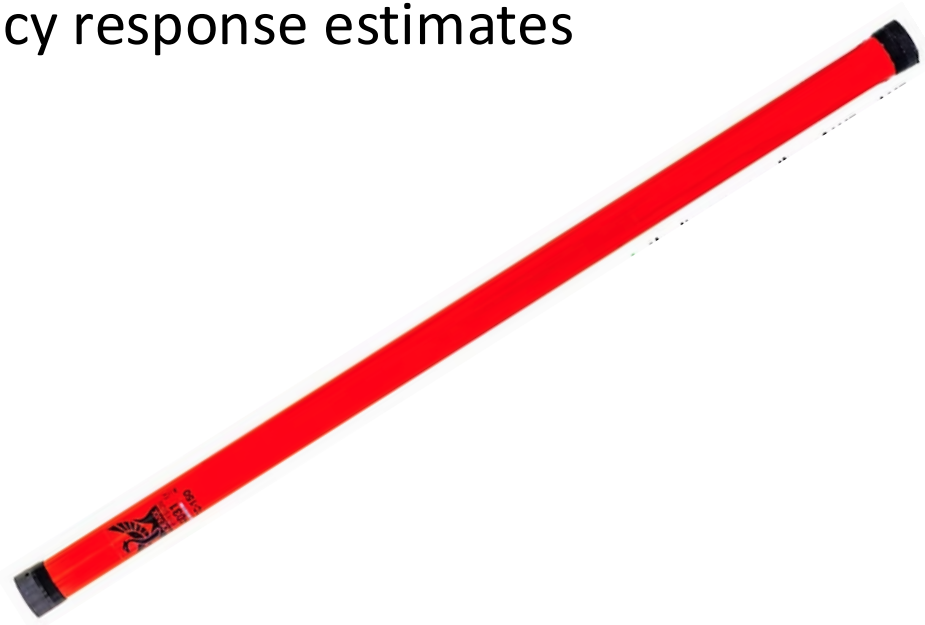

Acquisition – Innovative e-field acquisition

To enhance very low e-field signal at < 0.1 Hz, Phoenix designed an electric field combiner effectively increasing dipole length to 400m.

Acquisition time increased up to 4 days (3 nights) at most sites.

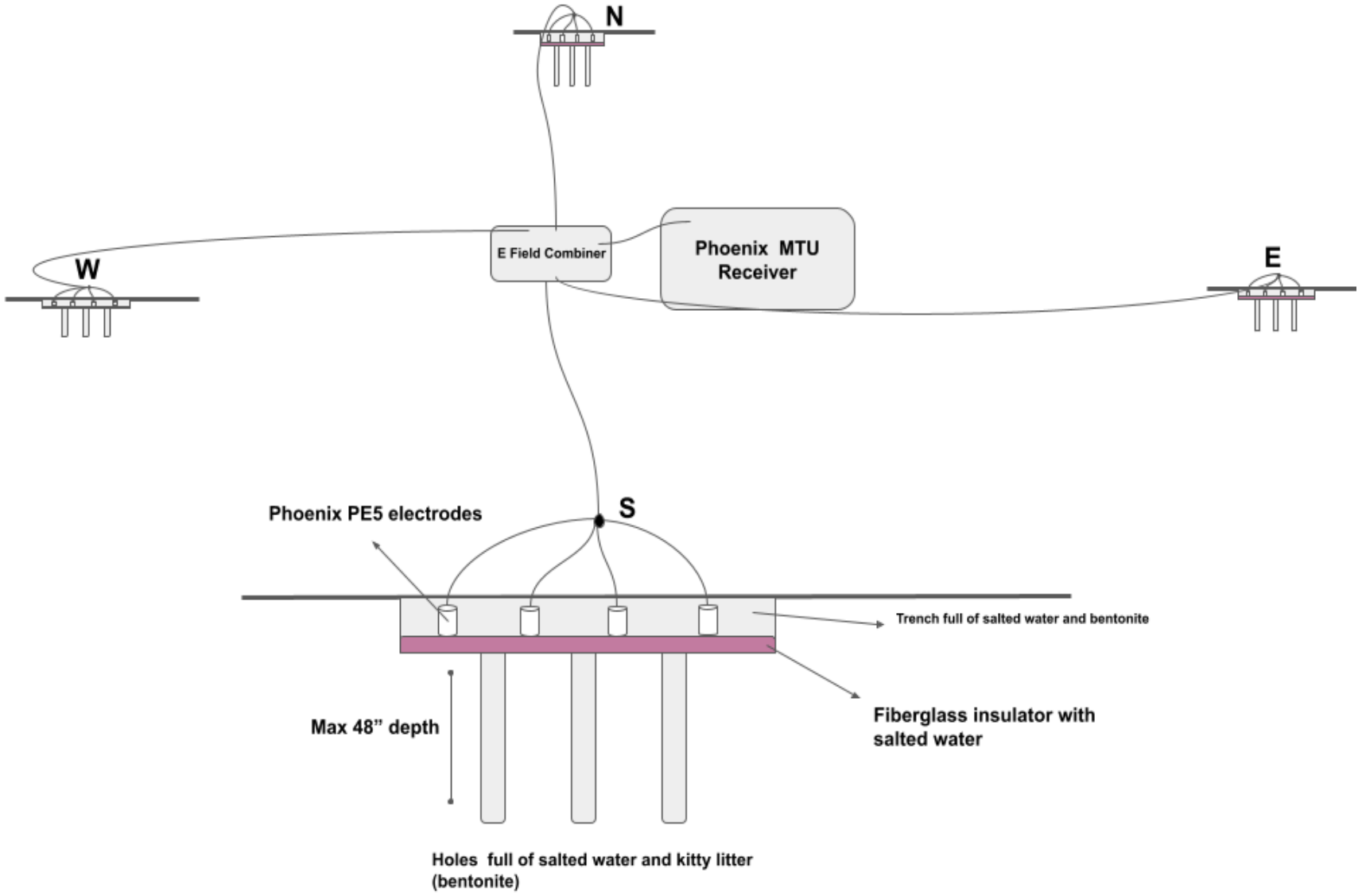

Acquisition – Innovative e-field acquisition

Comparison of MT estimates for a single pot (black) to a combiner (red) at the same site and same time at the commencement of Phase II

Single pot estimates fall apart < 1 Hz. Combiner results extend to lower frequencies and are very promising

Note: These are Field EDIs, so no remote-referencing or post-processing

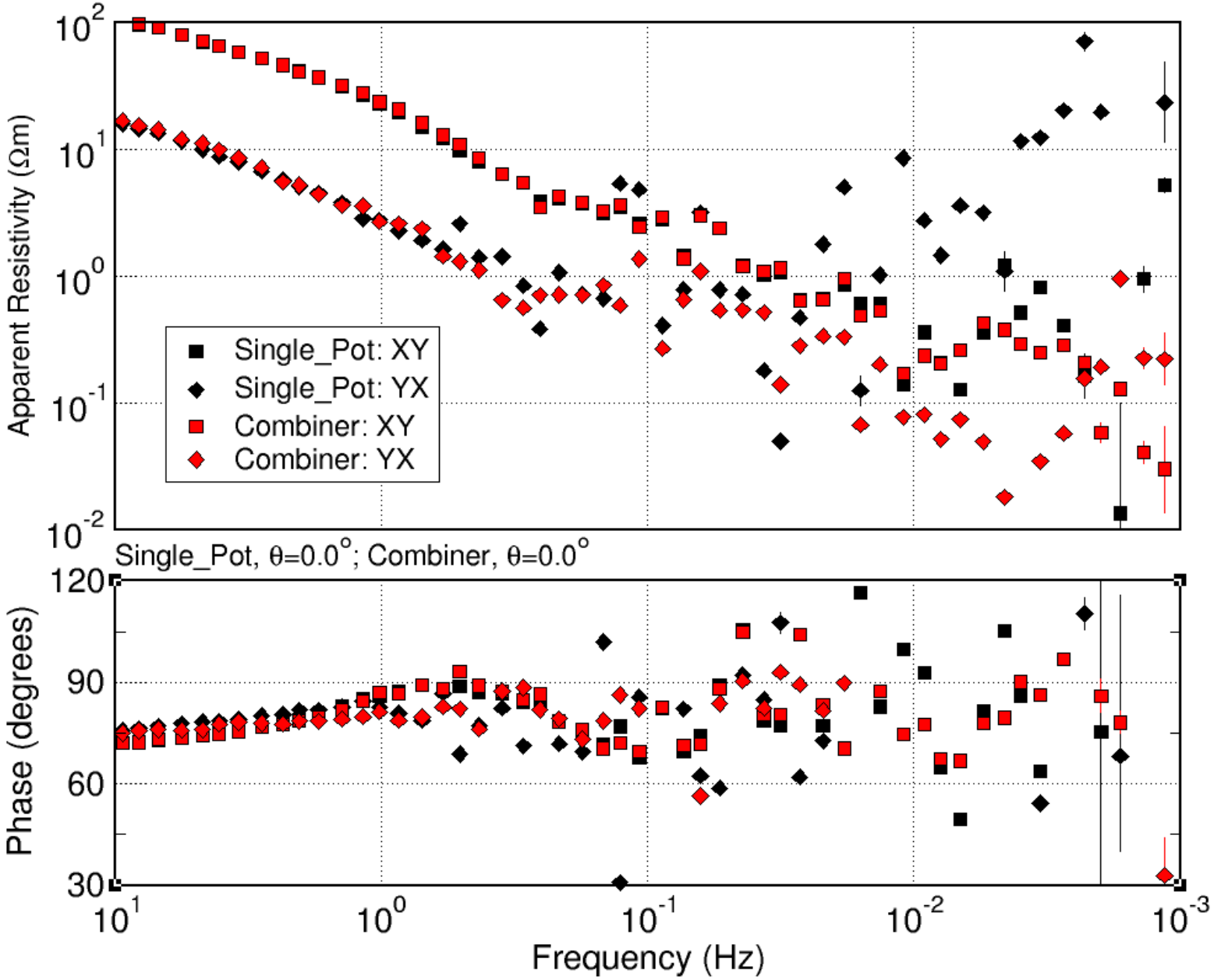

Acquisition – Low frequency signal – Kp indices

Bartel's K index is a 3-hour measure of magnetic activity on a logarithmic scale

Kp is the average of K values from 13 mid-latitude observatories across the planet

Kp	Amplitude (nT)
2	14
4	54
6	160
8	414

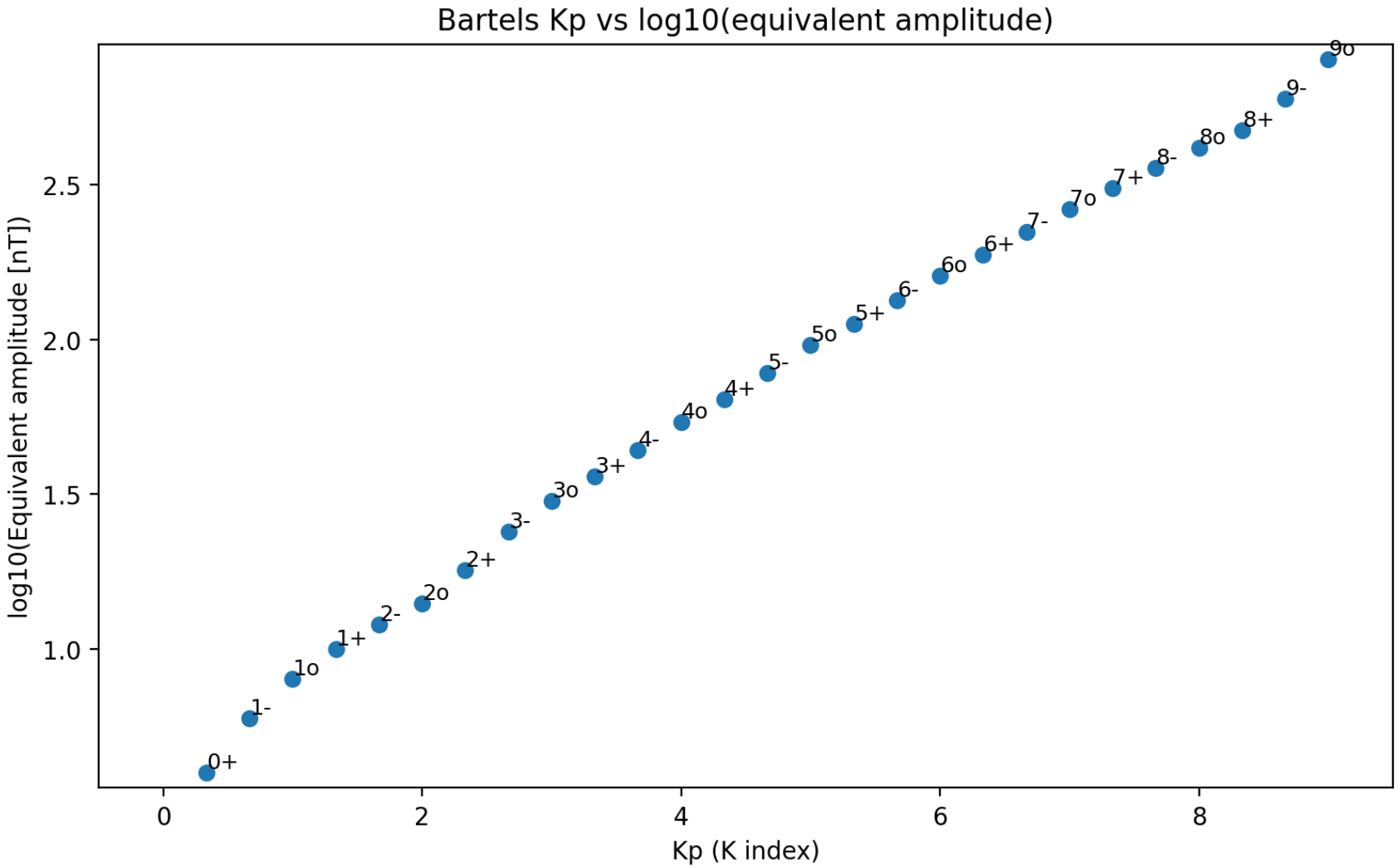

Acquisition – Low frequency signal – Kp indices

Planetary Kp indices for each phase were reasonable, with means of 1.4, 2.7 and 2.0 and maxima of 5.0, 8.3 and 4.7 for each phase

Kp	Ampl (nT)
2	14
4	54
6	160
8	414

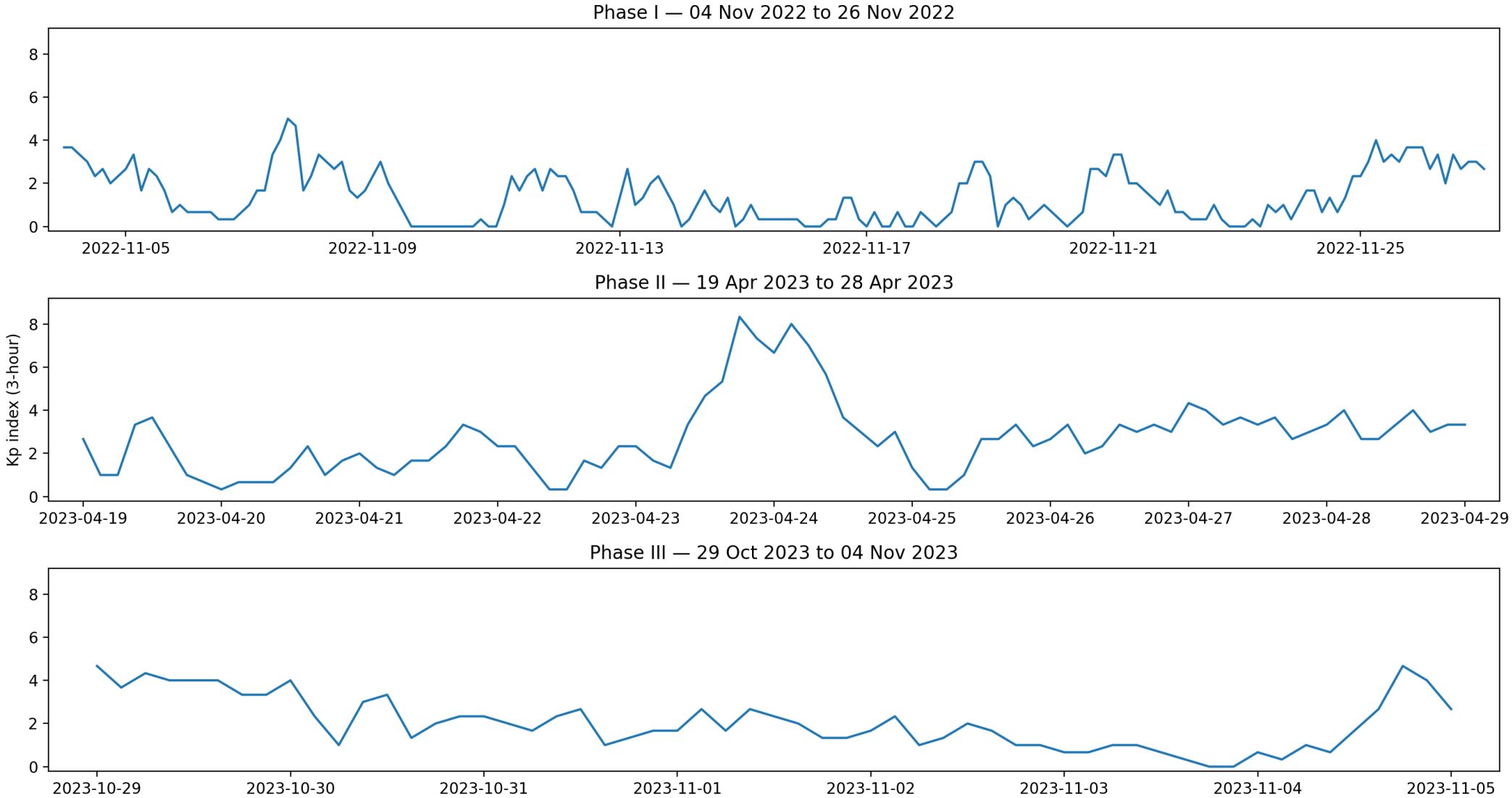

Acquisition – Comparison of MT estimates for high and low Kp

Plot of sites against Kp shows site MT-32 was recording during the massive magnetic storm!

Site MT-18 was recorded during a quieter period

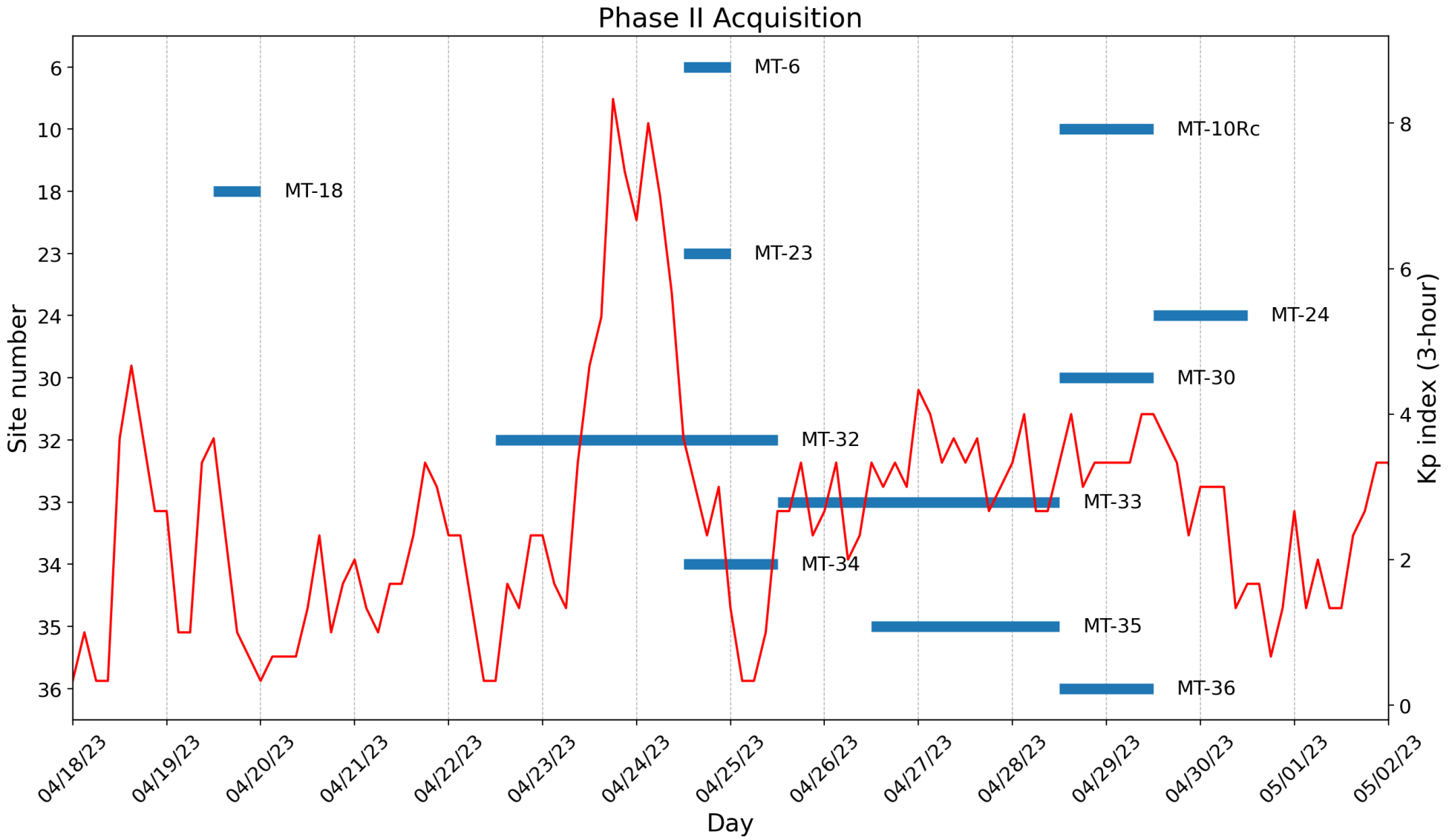

Acquisition – Comparison of MT estimates for high and low Kp

For MT-18 estimates (black) are very good quality only down to 0.01 Hz (100 s).

Low frequency estimates for MT-34 (red) very good quality down to 0.002 Hz (500 s), where RhoYX = 0.003 Ωm !!!

Normally the cut-off for high quality MT data is 1 Ωm

*** NOW is a great time to be acquiring low frequency MT data. We are coming off Solar Cycle 25 and the Sun will be much quieter by 2030 ***

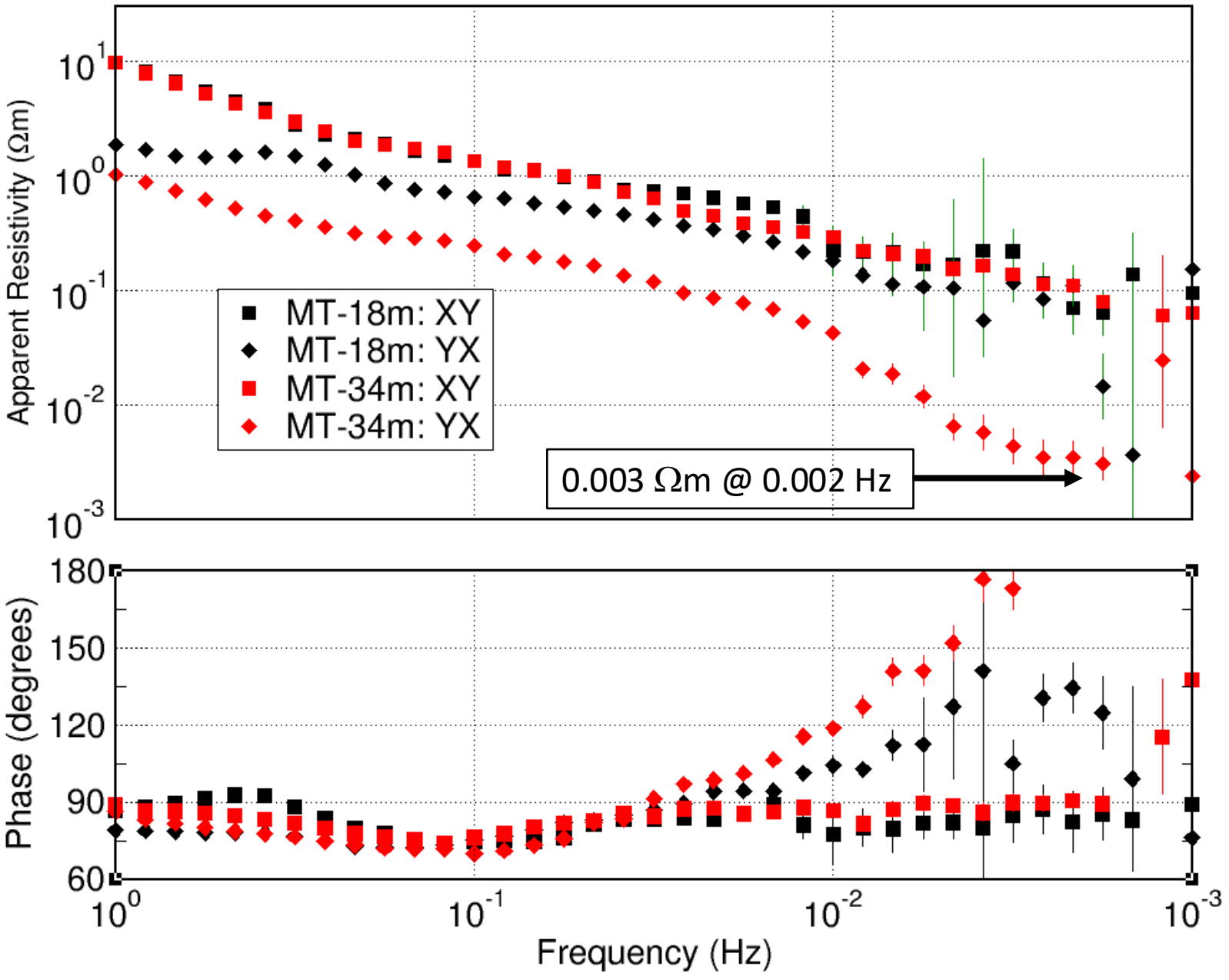

Processing - Phoenix

Phoenix processing (EMPower) is based on cascade decimation of the time series (Wight & Bostick, 1980), Least Trimmed Squares (LTS) robust processing (Jones & Joedicke, 1984),and interactive visual combining of windowed cross-spectral estimates.

Errors are calculated using a parametric estimator (Stodt, 1983).

CASCADE DECIMATION - A TECHNIQUE FOR REAL TIME ESTIMATION OF POWER SPECTRA

D. E. Wight
Hewlett-Packard Company
Ft. Collins, Co. 80525

F. X. Bostick
Electrical Engineering Dept.
The University of Texas
Austin, Tx. 78712

Magnetotelluric Transfer Function Estimation Improvement by a Coherence-Based Rejection Technique **EM1.5**

Alan G. Jones, Energy, Mines and Resources Canada; and Hartmut Jödicke, Westfalen Wilhelms Univ., West Germany

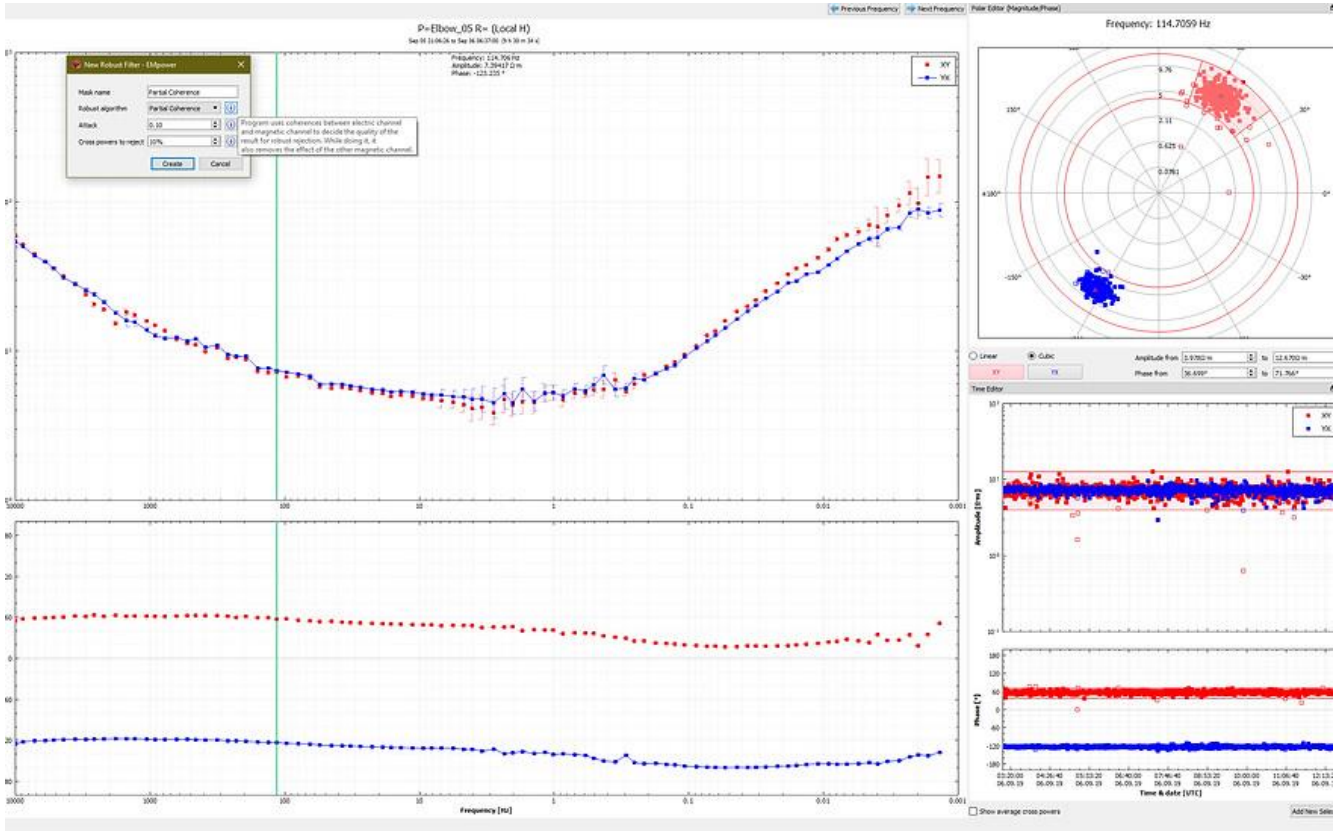

Processing - Viridien

Based on Larsen et al. (1996) - Robust estimates of the MT impedances are derived using an iterative frequency- and time-domain reweighted method on time series data corrected for outliers and gaps.

Errors are calculated using jackknife estimates of the solution covariance.

Geophys. J. Int. (1996) **124,** 801–819

Robust smooth magnetotelluric transfer functions

Jimmy C. Larsen,[1] Randall L. Mackie,[2] Adele Manzella,[3] Adolfo Fiordelisi[4] and Shirley Rieven[2]

[1] *Pacific Marine Environmental Laboratory, National Oceanic and Atmospheric Administration, 7600 Sand Point Way NE, Seattle* WA 98115-0070 *USA*
[2] *Massachusetts Institute of Technology, 42 Carleton Street, Cambridge, MA* 02142, *USA*
[3] *CNR-International Institute for Geothermal Research, Piazza Solferino 2, Pisa* 56126, *Italy*
[4] *ENEL, Esplorazione Mineraria, Via Andrea Pisano,* 120 *Pisa* 56122, *Italy*

High frequency Quality Factors: 10 kHz – 1 Hz

Objective Quality Factors of MT estimates based on smoothness and errors
QF=1 means data are smooth with errors within defined error bounds, set to 3.5% on RhoA and 2º in phase

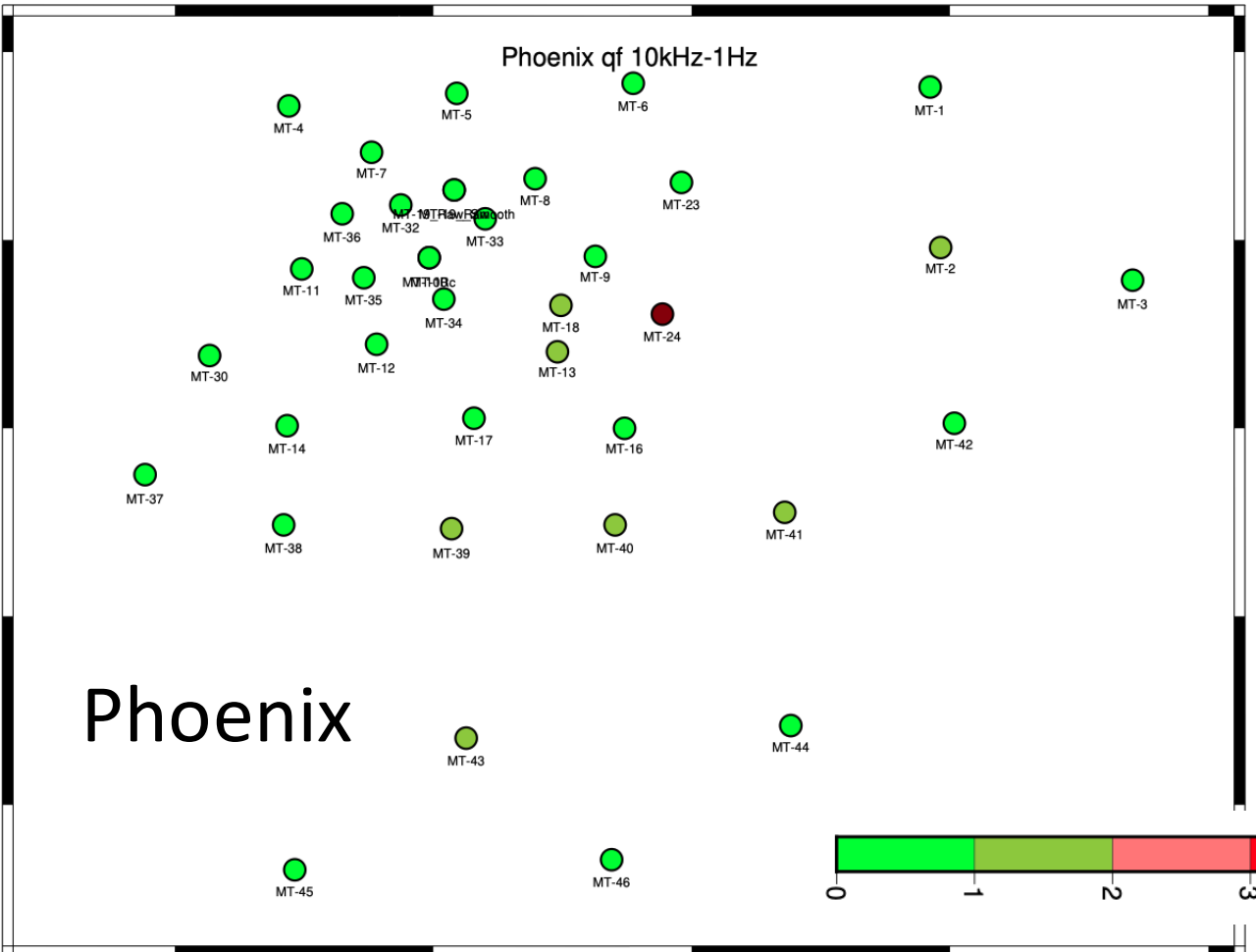

Phoenix

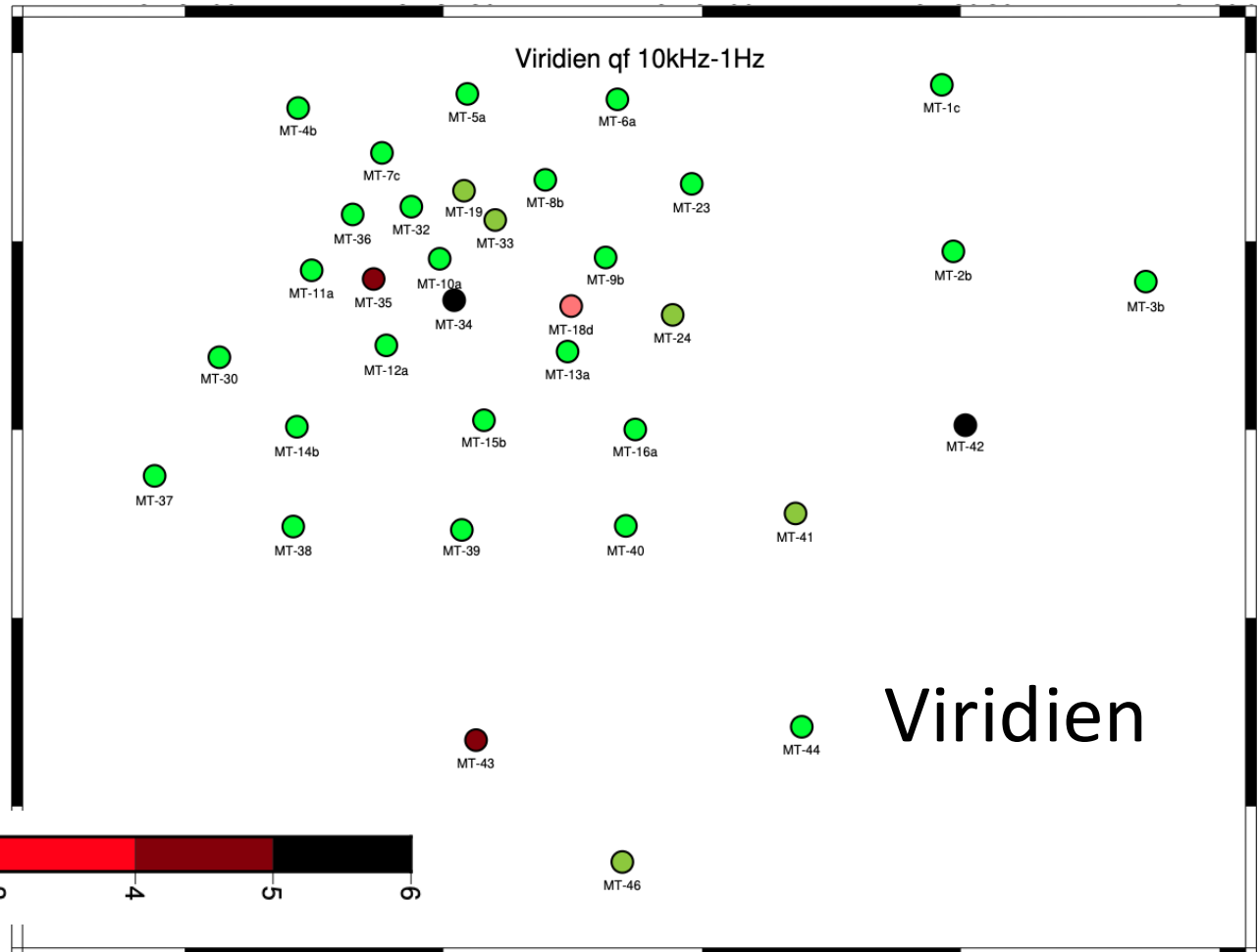

Viridien

Low frequency Quality Factors: 1 Hz – 0.01 Hz

Objective Quality Factors of MT estimates based on smoothness and errors
QF=1 means data are smooth with errors within defined error bounds, set to 3.5% on RhoA and 2º in phase

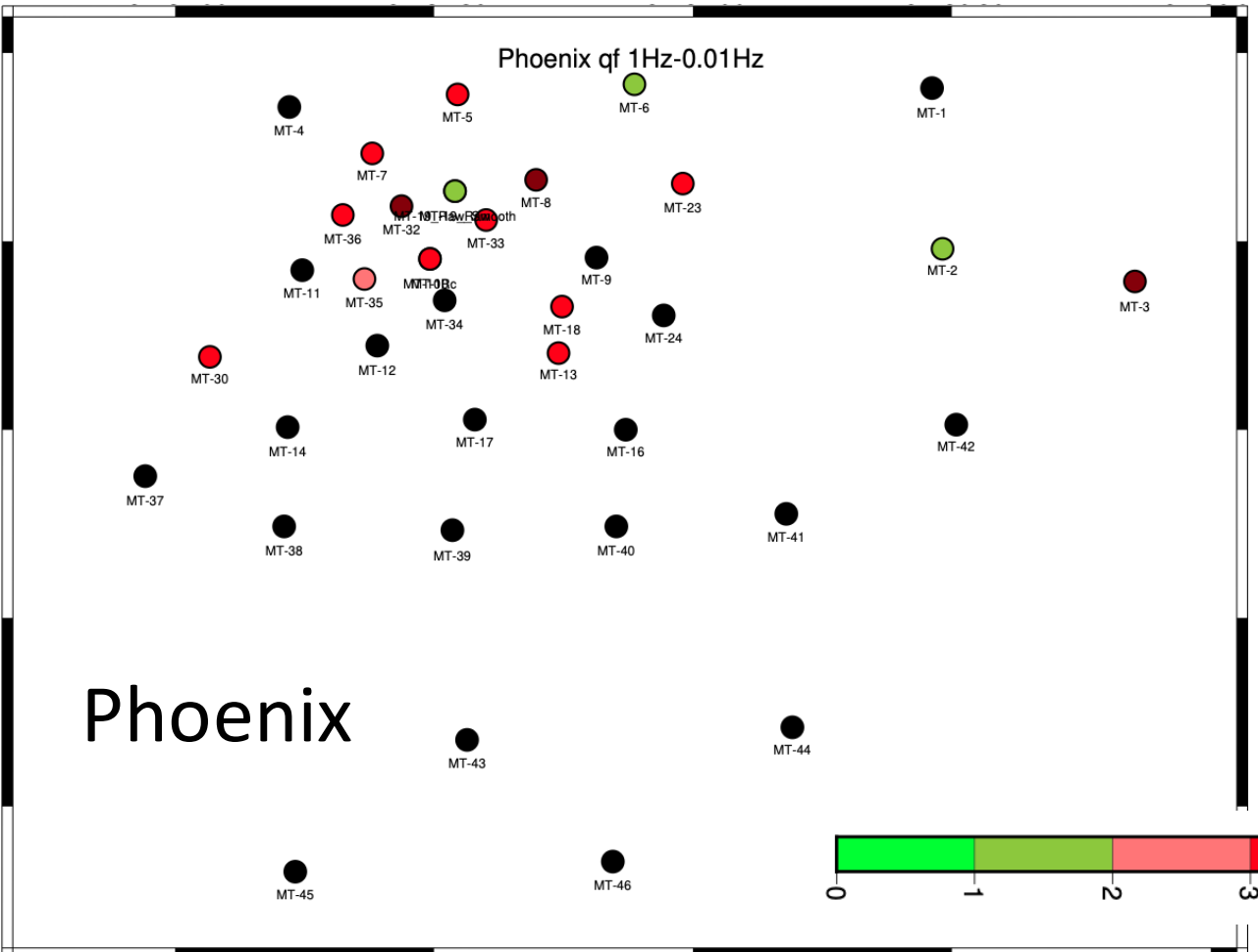

Phoenix

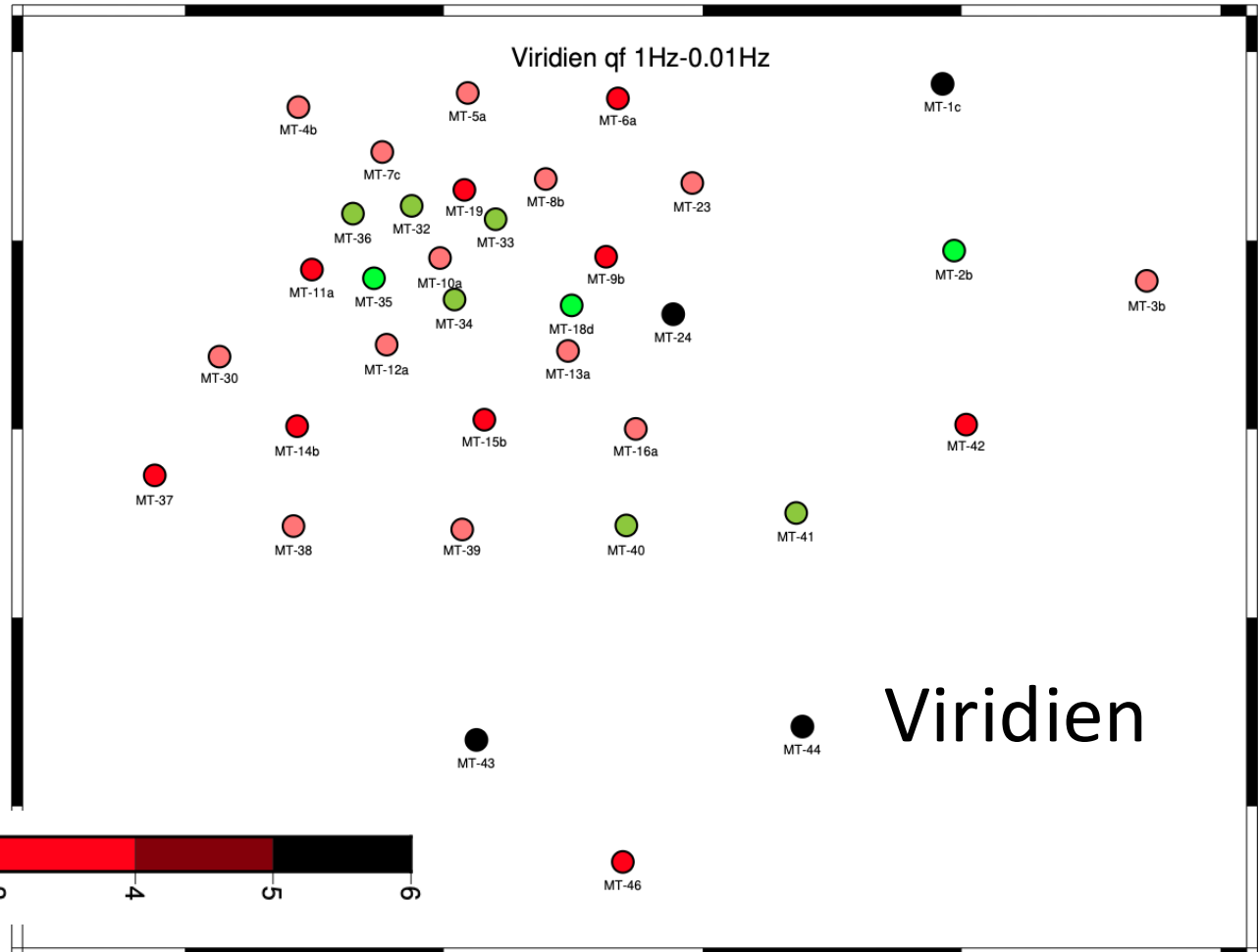

Viridien

Low frequency Quality Factors: 1 Hz – 0.01 Hz

Objective Quality Factors of MT estimates based on smoothness and errors
QF=1 means data are smooth with errors within defined error bounds, set to 3.5% on RhoA and 2º in phase

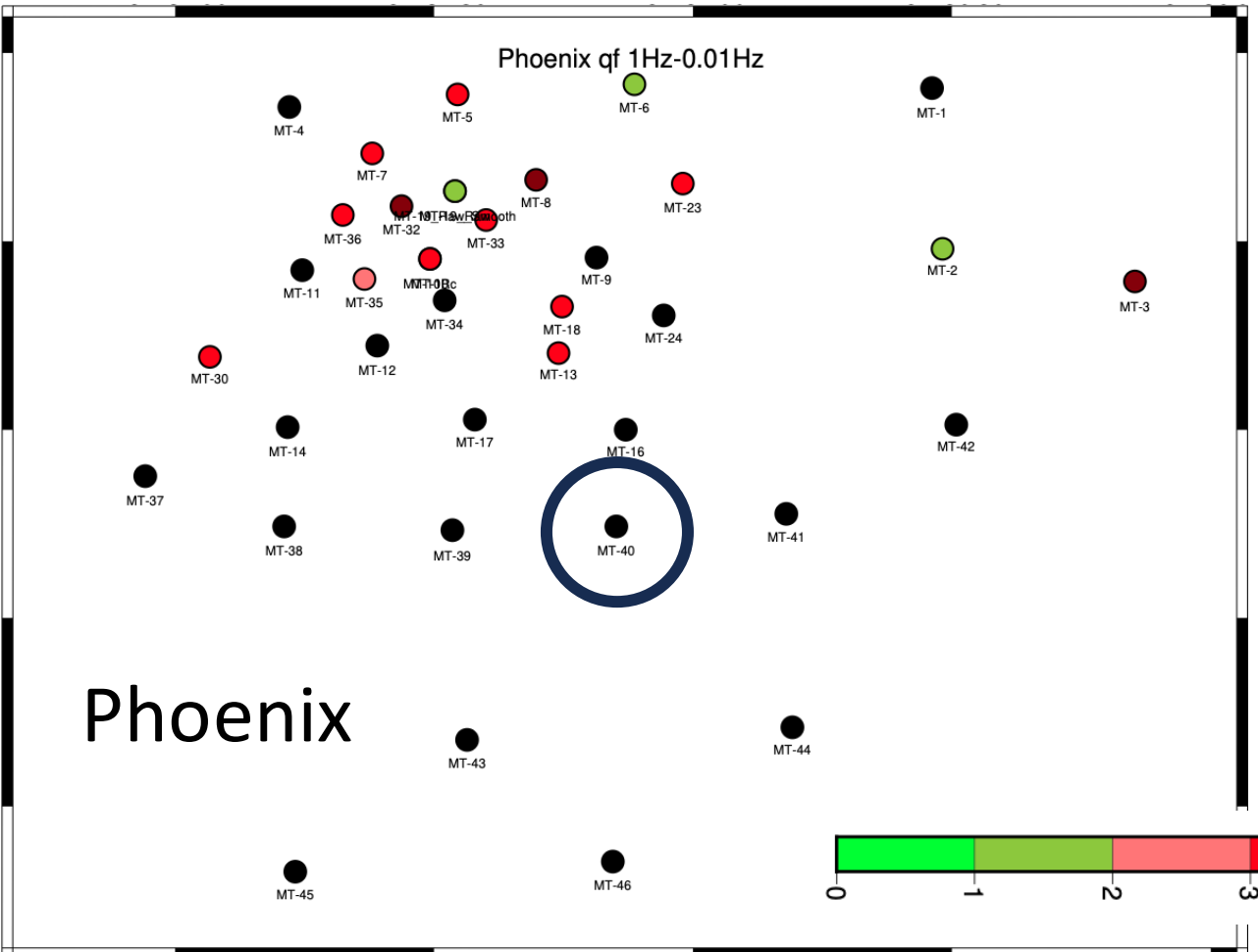

Phoenix

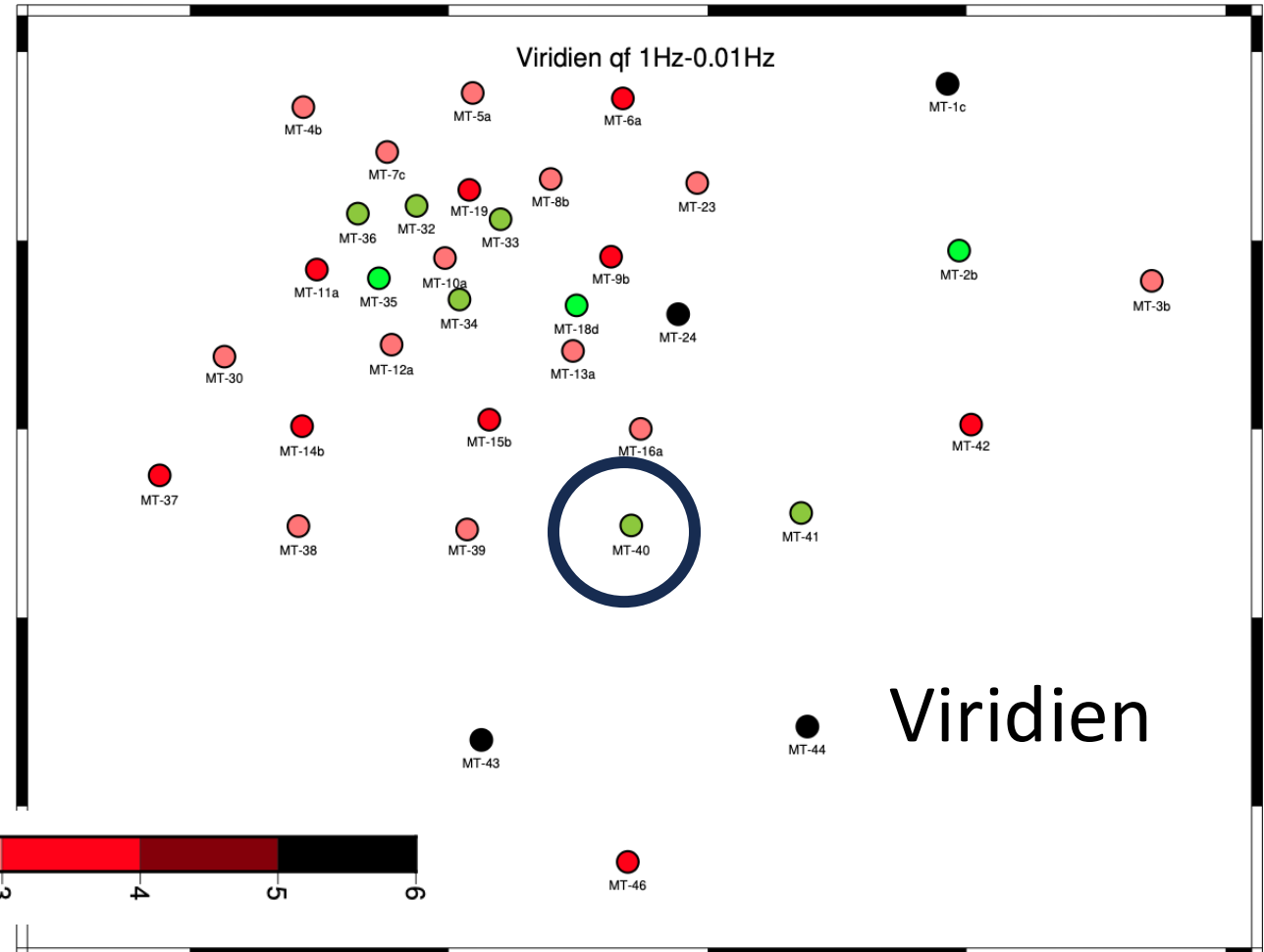

Viridien

Site MT-40

Comparison of processing at Phase III site MT-40 – most extreme case

Black: Phoenix

Red: Viridien

Basement information below ~0.1 Hz

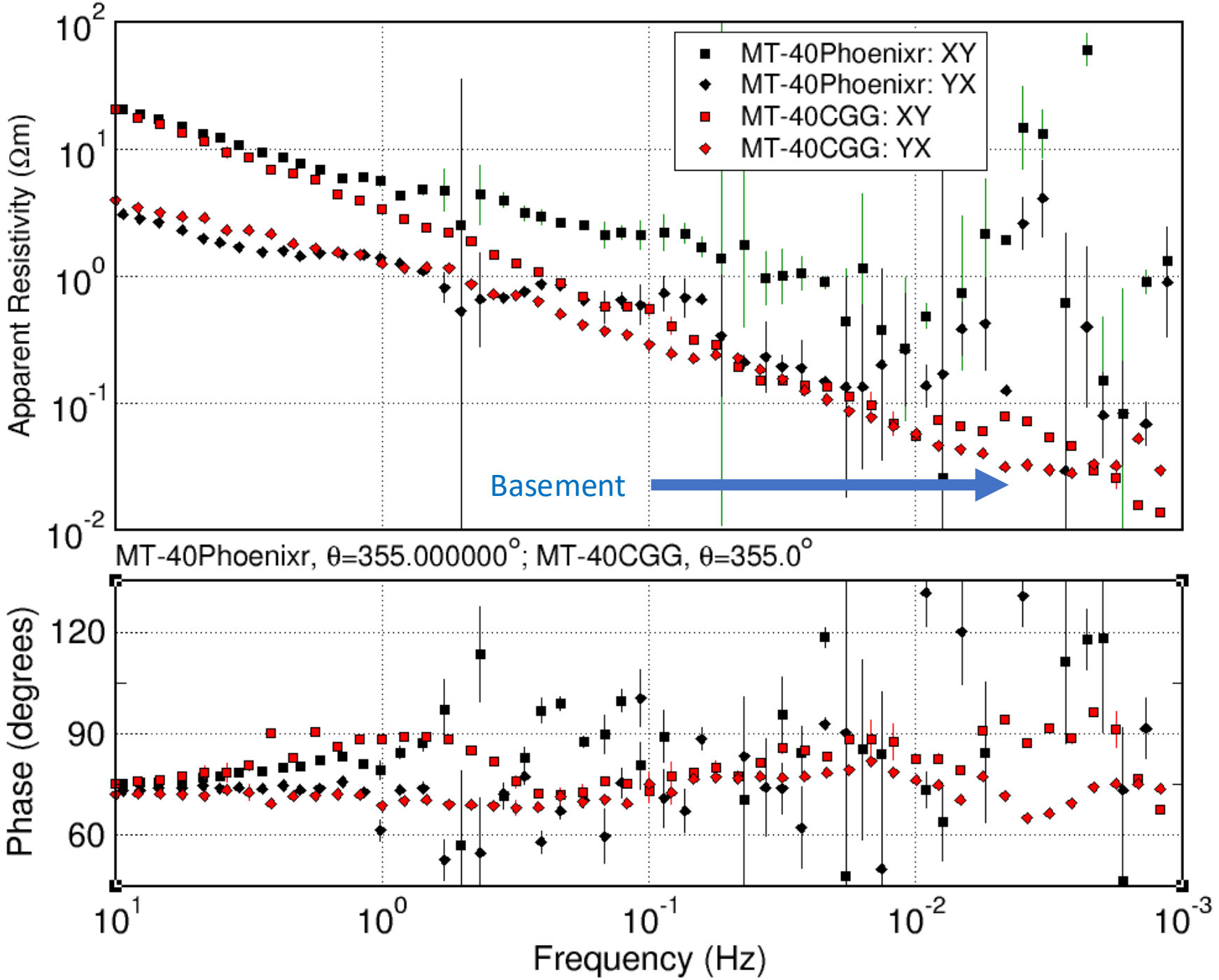

Processing – Splicing & Editing

The Phoenix data and Viridien data were spliced, taking the Phoenix estimates at high frequencies and the Viridien estimates at low frequencies.

The splice frequency was data-defined to give the lowest QF possible.

The spliced data were then visually edited to remove spurious outliers.

Phase II splice →

Site	Ph	Viridien	Splice frequency					
			30 Hz	10 Hz	3 Hz	1 Hz	0.3 Hz	0.1 Hz
MT-6	2.92	**0.82**	2.59	2.96	3.26	3.40	3.26	2.98
MT-10b	3.38	0.85	0.82	0.79	**0.73**	0.75	0.74	0.78
MT-18	2.34	1.21	**1.20**	1.24	1.40	1.53	1.40	1.24
MT-19	1.02	1.77	1.60	1.44	**1.37**	1.42	1.37	1.44
MT-23	4.09	1.78	1.78	1.77	1.76	**1.75**	1.76	1.77
MT-24	12.42	5.81	5.13	**4.98**	7.39	18.67	39.39	36.62
MT-30	3.36	1.98	1.98	1.96	1.95	**1.94**	1.95	1.96
MT-32	4.48	1.39	1.38	1.37	1.36	**1.35**	1.36	1.37
MT-33	2.87	1.54	1.55	1.50	1.48	**1.48**	1.48	1.50
MT-34	6.24	1.27	1.28	1.28	1.15	**1.09**	1.15	1.29
MT-35	2.19	0.83	0.87	0.86	0.86	**0.74**	0.86	0.86
MT-36	3.95	0.90	0.90	**0.89**	0.90	0.94	0.91	0.92

Low frequency Spliced Edited data Quality Factors

Objective Quality Factors of MT estimates based on smoothness and errors

QF=1 means data are smooth with errors within defined error bounds, set to 3.5% on RhoA and 2^{o} in phase

1 Hz – 0.01 Hz band

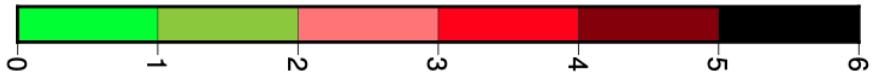

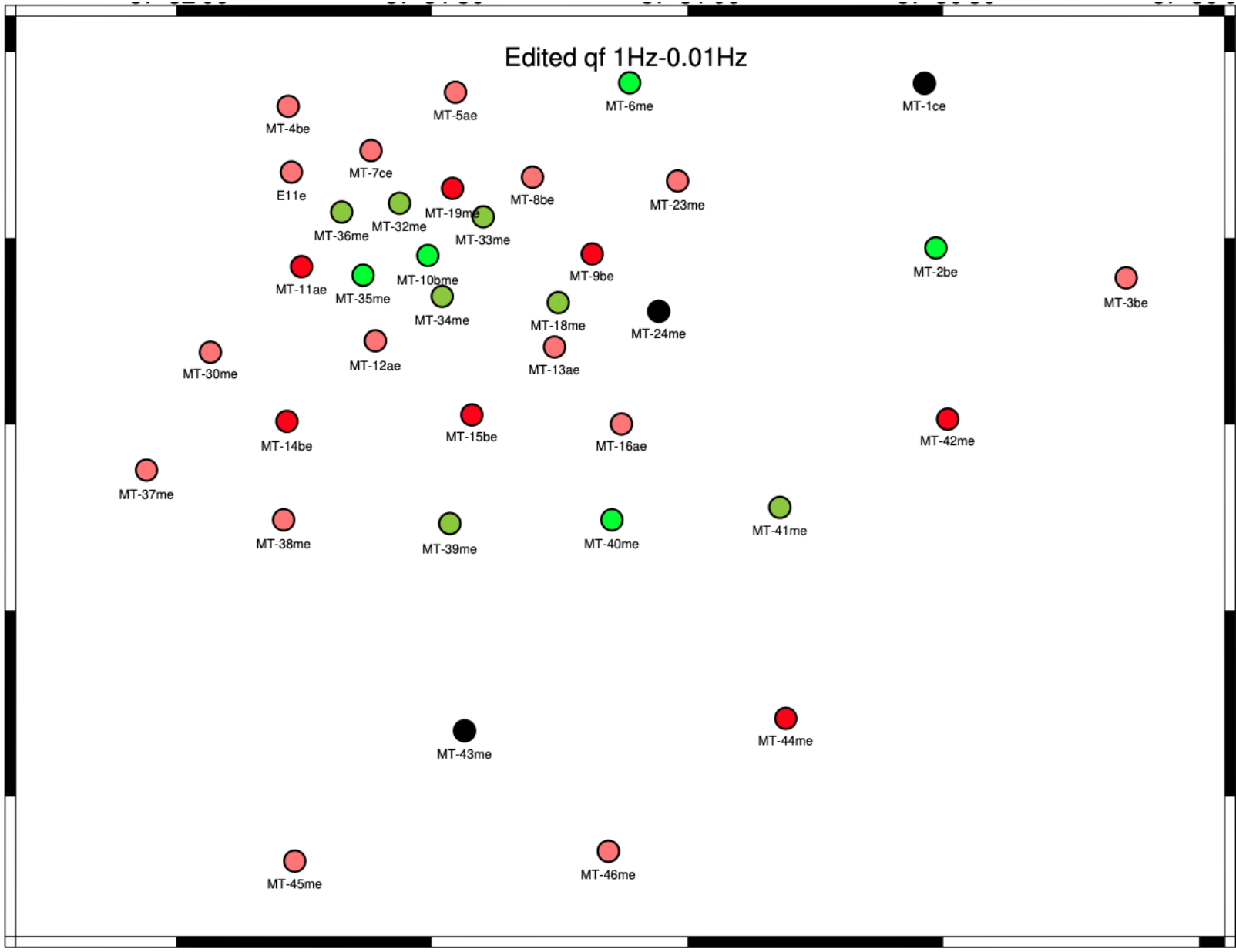

Inversion – 3-D code innovations

This project was able to take advantage of new functionality developed by Mackie (Viridien) in his RLM-3D inversion code

1) Instead of inverting the complex impedances, Z, RLM-3D can optionally invert the log amplitude and phase of the off-diagonal impedance elements (Zxy and Zyx). Inversion for the real and imaginary parts of the diagonal elements (Zxx and Zyy) is maintained, since those can be very small, especially at higher frequencies, and are typically down-weighted relative to the off-diagonal impedances.

2) A weighting factor was added to tear surfaces, to allow tears to either be ignored (weight = 0) or to allow unpenalised sharp boundary at the tears (weight = 1)

Inversion – 3-D inversion runs

Multiple inversion runs after each Phase using:

Data:

- Different data types – MT full **Z** only, MT Zxy+Zyx only, MT+Tipper (TE+TM+TZ)
- Different number of data per decade, varying number of data per decade
- Different error floors

Inversion:

- Different inversion parameters; horizontal and vertical smoothing, Tikhonov trade-off parameter
- Different start models
- Different cell sizes of the grids (“Model”)
- With and without tear surfaces, & changing tear weighting
- Inverting Z or RhoA/Pha

Inversion – 3-D inversion runs

Phase I	No. of runs
Model01	12
Model02	1
Model03	3

Phase II	No. of runs
Model04	12
Model05	8

Phase III	No. of runs
Model06	4
Model07	8
Model08	2
Model09	9
Model10	5

Each run for each Model (=different grid) was typically 50-100 iterations – runs were monitored and ended if RMS & ObjFn asymptoted or the run was stalled
Some runs were dead-ends, some yielded information that were used in the successive runs

Inversion – Best model to date - Model10Run04Iter50

Two 3-D views of the model, from above and from the South

No tear surfaces in this model. Final total misfit nRMS = 2.13

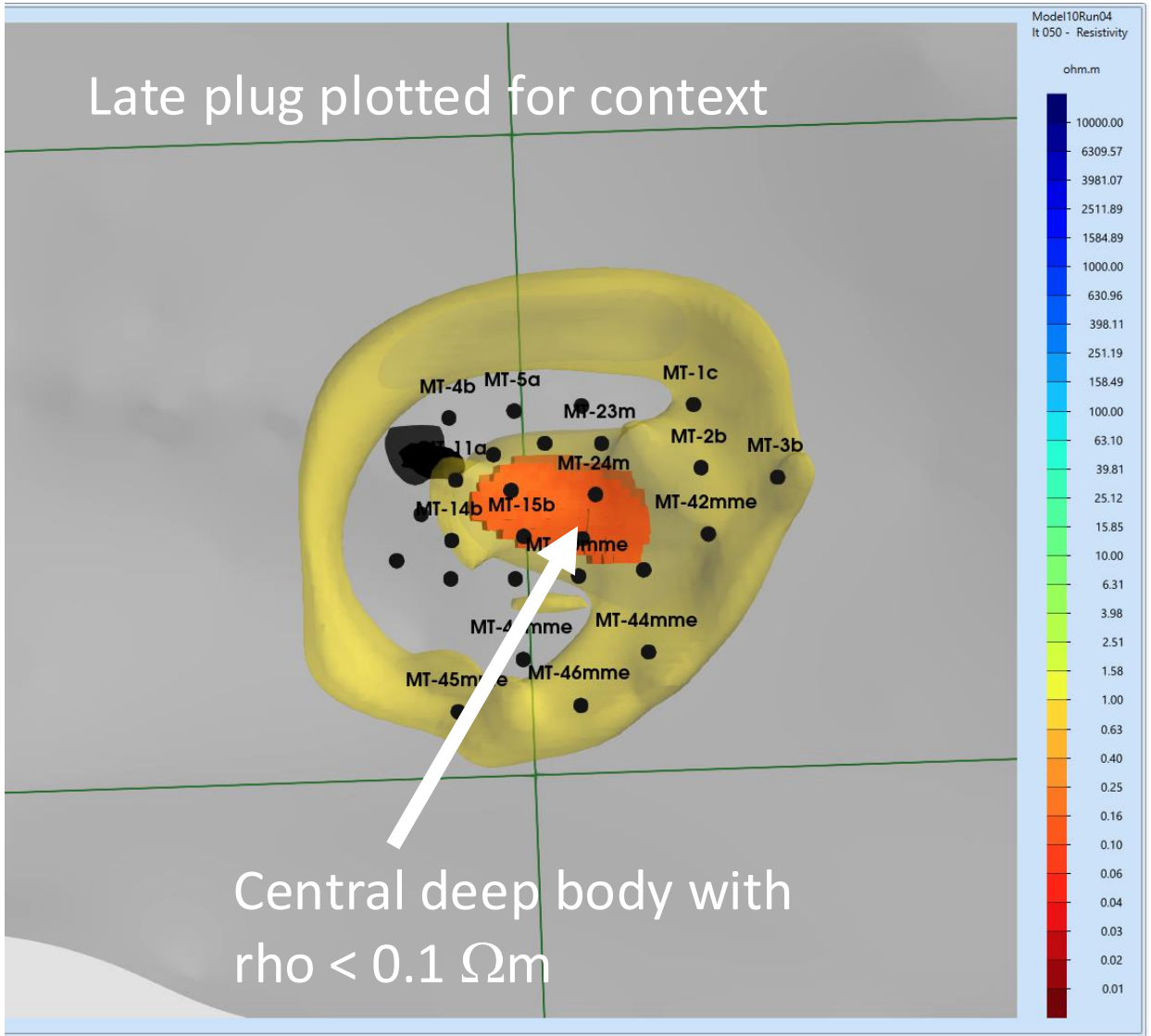

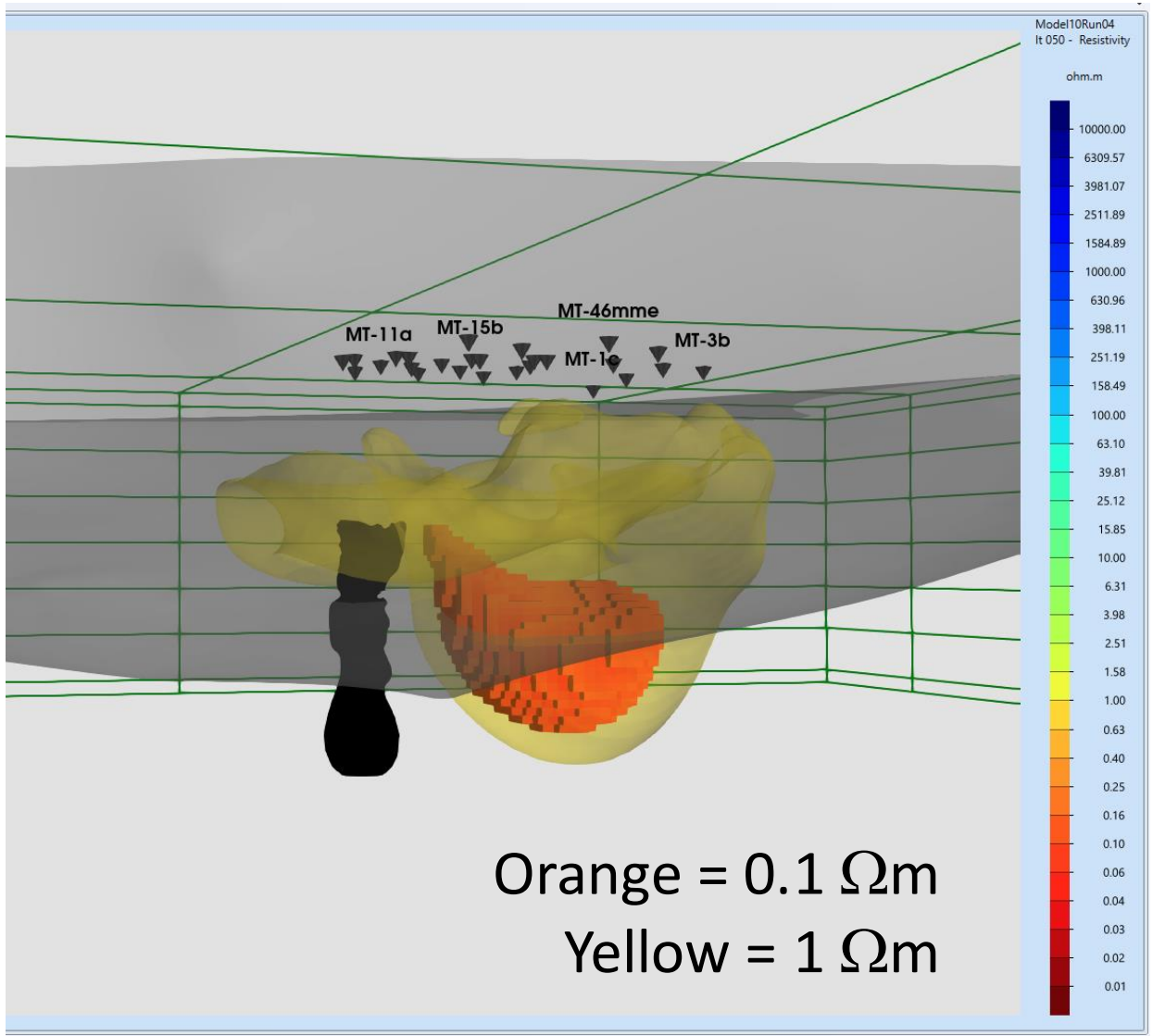

Inversion – Best model – basement core

The central conductor has a core of rho < 0.03 Ωm that has its top exactly at the basement surface

(no tear surface in this run)

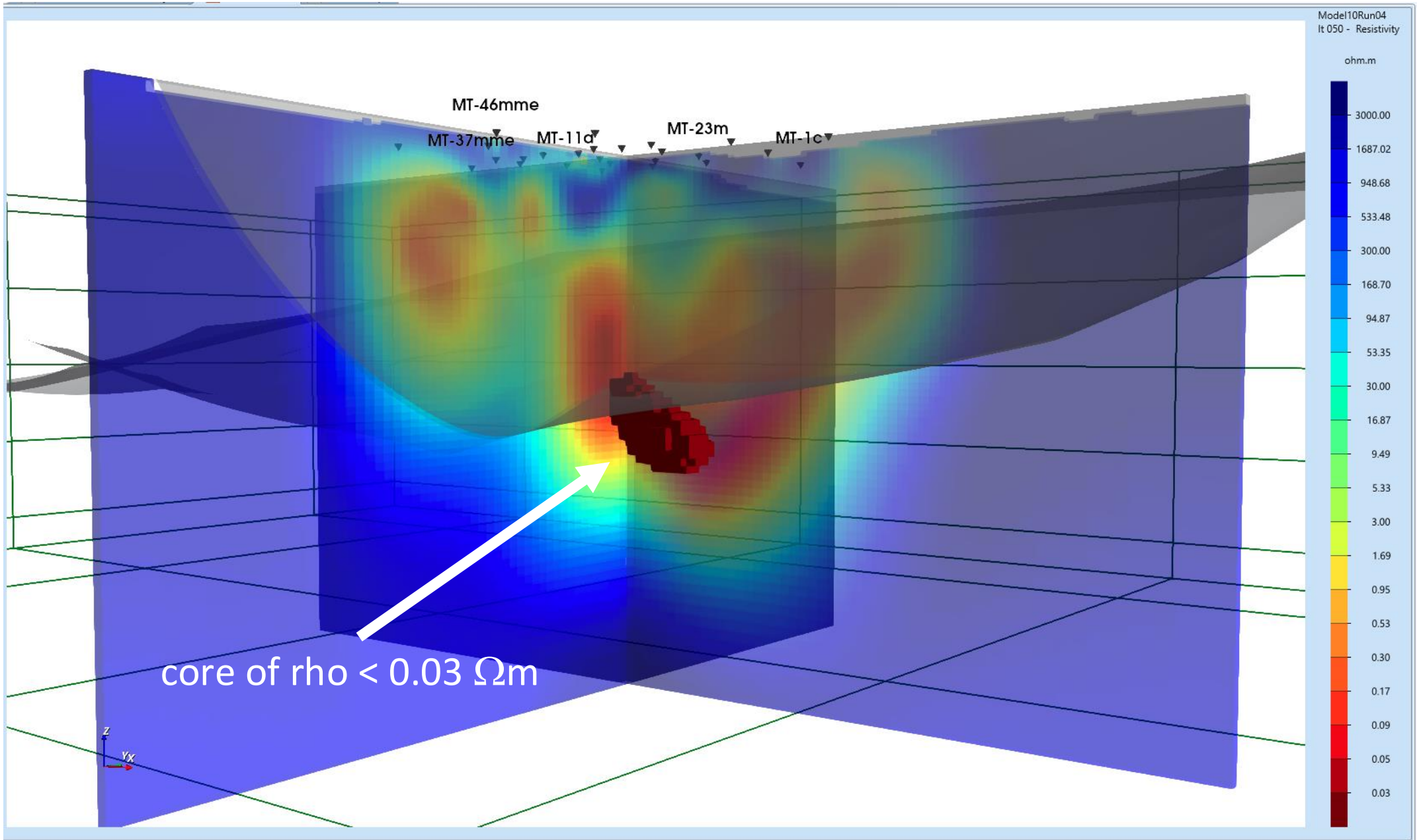

Inversion – Model station misfits

Station misfits to impedances (Z nRMS=1.90) and tippers (TZ, nRMS=2.37) show that some data are not adequately explained by the model, especially the TZ

(Assigned errors: 5% on ZXY & ZYX; 100% on ZXX & ZYY; 0.02 on Tippers)

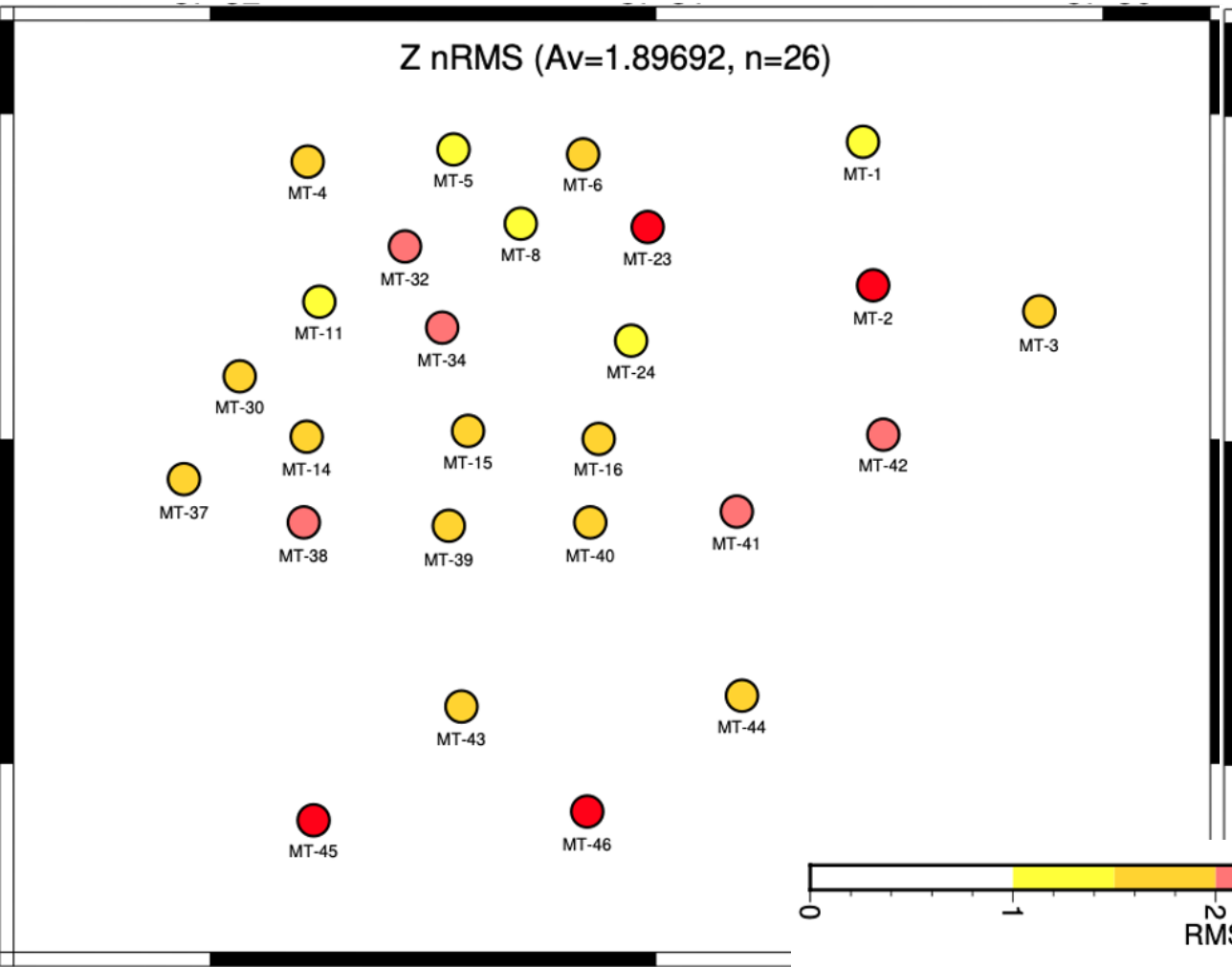

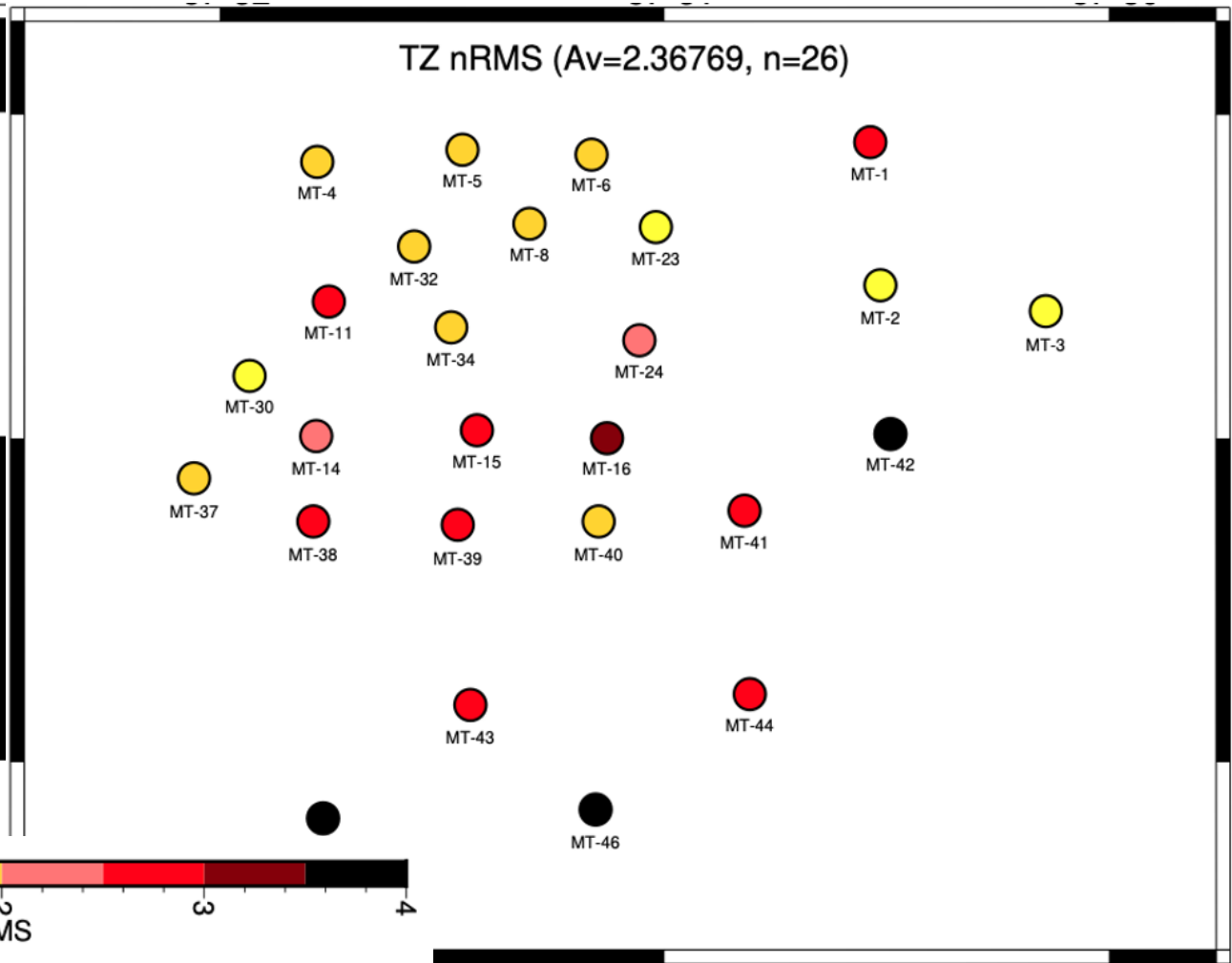

Inversion – Model frequency misfits

Misfits summed over all stations at the same frequency also show that some data are not adequately explained by the model, esp. at low freqs (<0.01 Hz in MT and 0.1 Hz in Tipper)

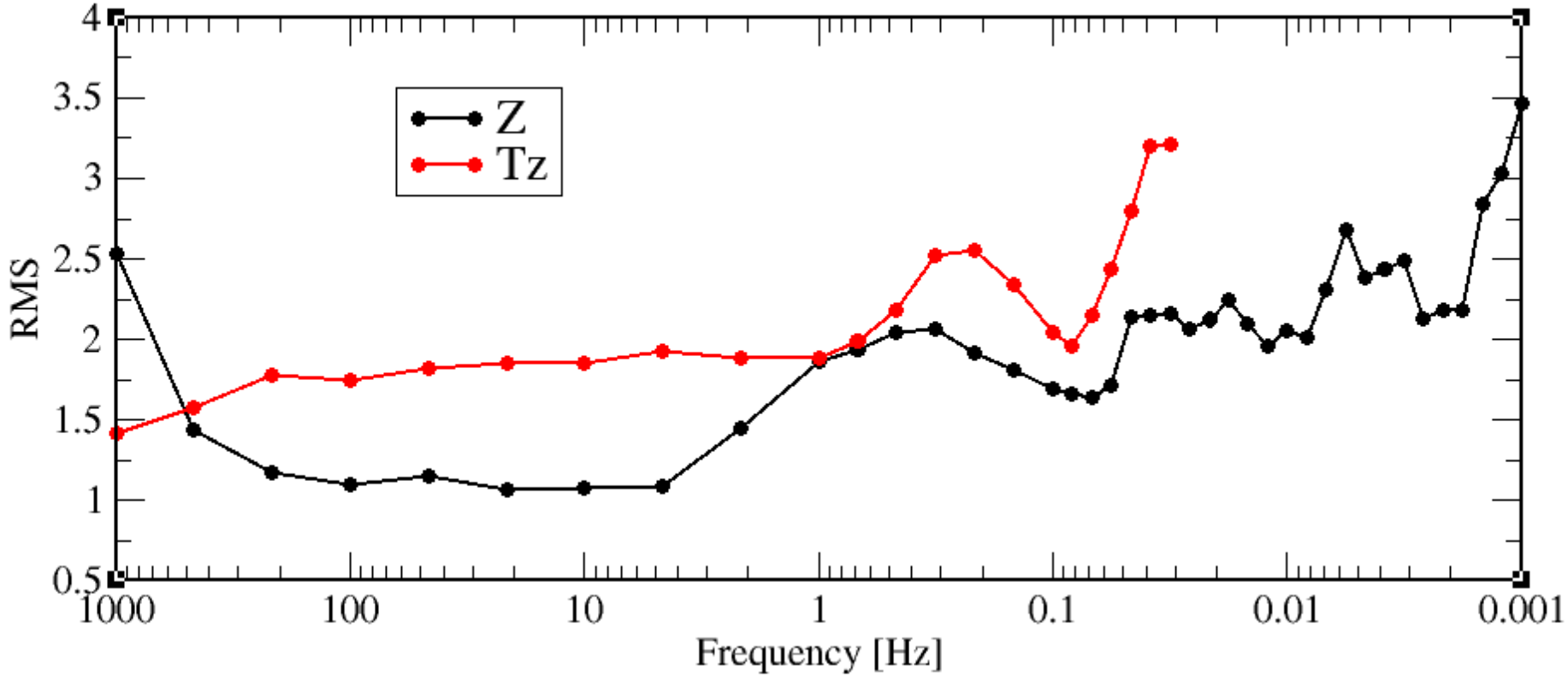

Assigned errors: 5% on ZXY & ZYX; 100% on ZXX & ZYY; 0.02 on Tippers

Final model implications

The MT 0.1 Ωm conductor lies down-dip of Eagle East and along strike of known mineralization

Drilling intersected a pyrrhotite-rich formational conductor

Exploration program ongoing

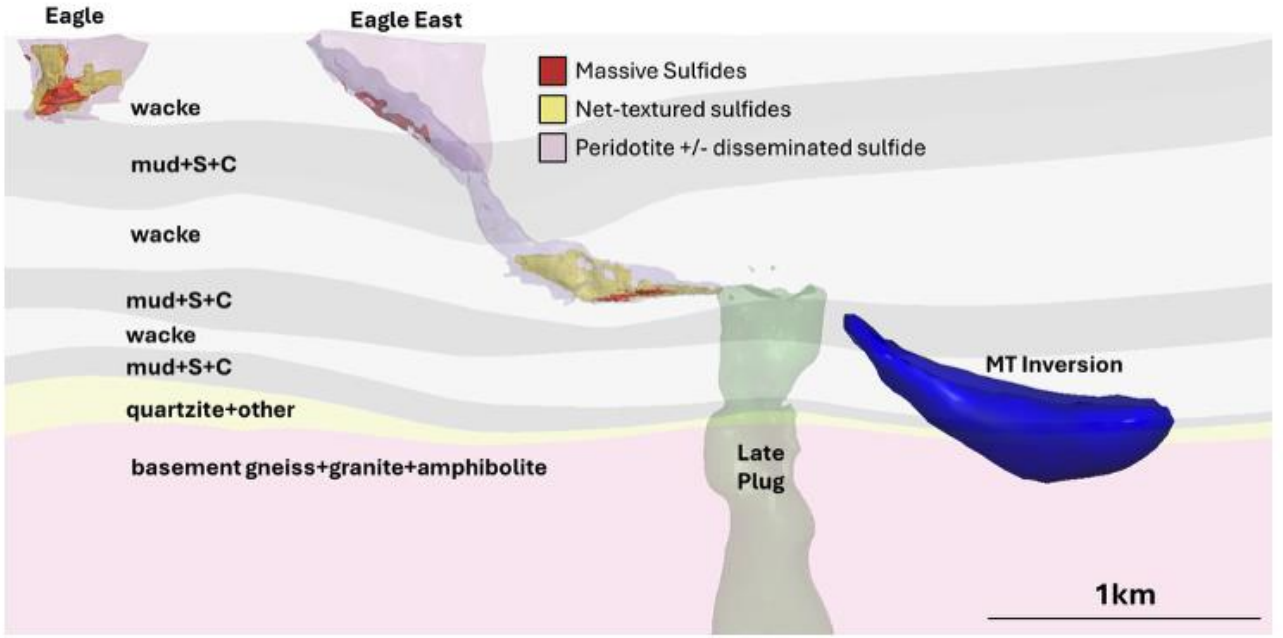

Long section looking north.

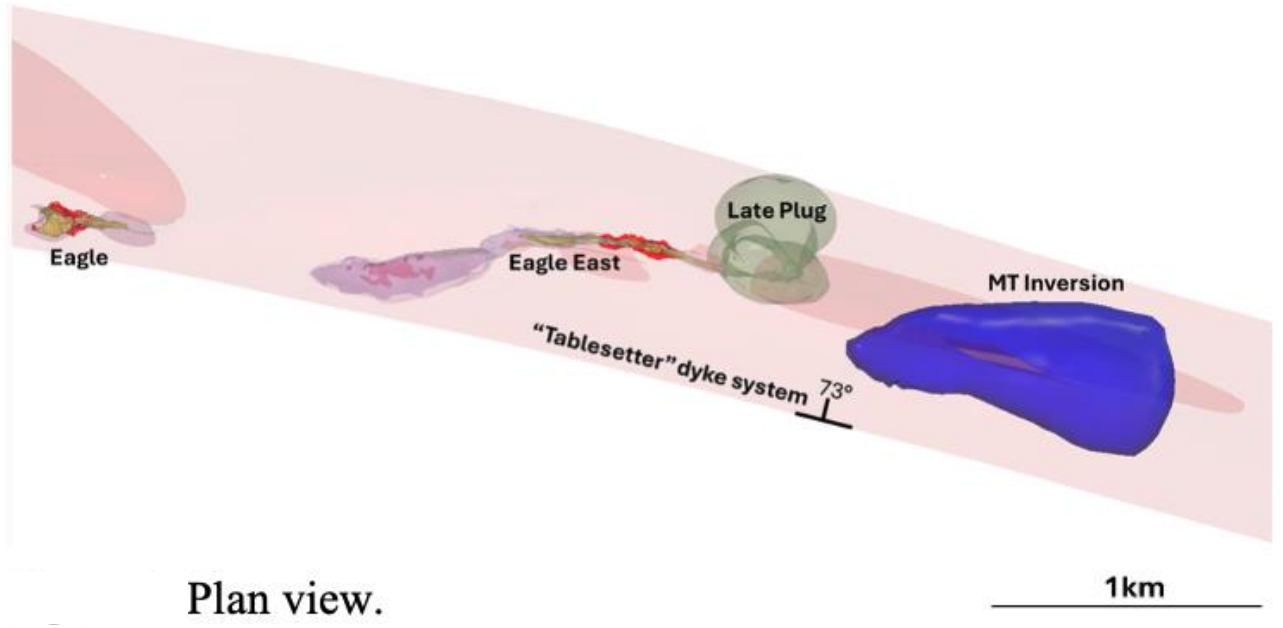

Plan view.

Conclusions

1) The primary objective – detecting the presence of conducting features in the basement – is extremely difficult to achieve given the highly conducting overlying sediments. The signal for basement conductors is at low frequencies <0.1 Hz where the RhoA data are below 0.1 Ωm.

Conclusions

1) The primary objective – detecting the presence of conducting features in the basement – is extremely difficult to achieve given the highly conducting overlying sediments. The signal for basement conductors is at low frequencies <0.1 Hz where the RhoA data are below 0.1 Ωm.
2) Extraordinary effort was made by all involved: By Phoenix Geophysics to acquire the very best possible data, by MTGS to assess the incoming data in near-real-time for dynamic survey design, by Viridien to obtain the very best response estimates, by MTGS, together with Viridien, to model the response estimates, and by Eagle Mine and Lundin Mining to support the intermediate outcomes by collecting additional data.

Conclusions

1) The primary objective – detecting the presence of conducting features in the basement – is extremely difficult to achieve given the highly conducting overlying sediments. The signal for basement conductors is at low frequencies <0.1 Hz where the RhoA data are below 0.1 Ωm.
2) Extraordinary effort was made by all involved: By Phoenix Geophysics to acquire the very best possible data, by MTGS to assess the incoming data in near-real-time for dynamic survey design, by Viridien to obtain the very best response estimates, by MTGS, together with Viridien, to model the response estimates, and by Eagle Mine and Lundin Mining to support the intermediate outcomes by collecting additional data.
3) Three novel inversion tactics were adopted to require the code to fit the faint signal at the low frequencies:
   a) On final runs more low frequency data were inverted, with 3 pts/decade from 1 kHz – 1 Hz, 6 pts/decade from 1 Hz – 0.1 Hz, and 12 pts/decade from 0.1 Hz – 0.001 Hz.
   b) Errors, not error floors, were adopted. This emphasized fit to the low frequency estimates.
   c) Stations were omitted to give a balanced coverage with approximately equal station spacing.

Conclusions

1) The primary objective – detecting the presence of conducting features in the basement – is extremely difficult to achieve given the highly conducting overlying sediments. The signal for basement conductors is at low frequencies <0.1 Hz where the RhoA data are below 0.1 Ωm.
2) Extraordinary effort was made by all involved: By Phoenix Geophysics to acquire the very best possible data, by MTGS to assess the incoming data in near-real-time for dynamic survey design, by Viridien to obtain the very best response estimates, by MTGS, together with Viridien, to model the response estimates, and by Eagle Mine and Lundin Mining to support the intermediate outcomes by collecting additional data.
3) Three novel inversion tactics were adopted to require the code to fit the faint signal at the low frequencies:
   a) On final runs more low frequency data were inverted, with 3 pts/decade from 1 kHz – 1 Hz, 6 pts/decade from 1 Hz – 0.1 Hz, and 12 pts/decade from 0.1 Hz – 0.001 Hz.
   b) Errors, not error floors, were adopted. This emphasized fit to the low frequency estimates.
   c) Stations were omitted to give a balanced coverage with approximately equal station spacing.
4) Despite all this effort, the data are weakly sensitive to the primary objective, and because of this weak sensitivity, the conductive basement feature shifts between final models depending on data selection, inversion parameters, and the presence or absence of tear surfaces.

Conclusions

1) The primary objective – detecting the presence of conducting features in the basement – is extremely difficult to achieve given the highly conducting overlying sediments. The signal for basement conductors is at low frequencies <0.1 Hz where the RhoA data are below 0.1 Ωm.
2) Extraordinary effort was made by all involved: By Phoenix Geophysics to acquire the very best possible data, by MTGS to assess the incoming data in near-real-time for dynamic survey design, by Viridien to obtain the very best response estimates, by MTGS, together with Viridien, to model the response estimates, and by Eagle Mine and Lundin Mining to support the intermediate outcomes by collecting additional data.
3) Three novel inversion tactics were adopted to require the code to fit the faint signal at the low frequencies:
   a) On final runs more low frequency data were inverted, with 3 pts/decade from 1 kHz – 1 Hz, 6 pts/decade from 1 Hz – 0.1 Hz, and 12 pts/decade from 0.1 Hz – 0.001 Hz.
   b) Errors, not error floors, were adopted. This emphasized fit to the low frequency estimates.
   c) Stations were omitted to give a balanced coverage with approximately equal station spacing.
4) Despite all this effort, the data are weakly sensitive to the primary objective, and because of this weak sensitivity, the conductive basement feature shifts between final models depending on data selection, inversion parameters, and the presence or absence of tear surfaces.
5) The final model is considered the best model that can be obtained at this time. It exhibits the lowest impedance misfit at the low frequencies.

Acknowledgements

The authors would like to thank Talon Metals and Eagle Mine for allowing us to present this story.

All authors would like to thank their respective organisations.

THANK YOU

CANADIAN EXPLORATION
GEOPHYSICAL SOCIETY